RENEWABLE ENERGY INTEGRATION IN CLOUD MANUFACTURING

FOR LOW CARBON OPERATIONS

by

Binbin Li

A thesis submitted to the Graduate Council of
Texas State University in partial fulfilment
of the requirement for the degree of
Master of Science in Technology
With a major in Industrial Technology
May 2015

Committee Members:

Tongdan Jin, Chair

Heping, Chen, Co-Chair

Vedaraman Sriraman

FAIR USE AND AUTHOR'S PERMISSION STATEMENT

Fair Use

Duplication Permission

DEDICATION

To my family, friends and people who ever helped me.

ACKNOWLEDGEMENTS

I would like to thank Dr. Tongdan Jin for what I have learned from him. I feel very fortunate to have someone like him to be my thesis mentor.

I would like to thank Dr. Heping Chen for his guidance in the field of machine learning, robotics and control system, from whom I learned a lot.

I would like to express my appreciation to Dr. Vedaraman Sriraman for teaching me the basics of research.

I want to thank Dr. Andy Batey, Dr. Stan McClellan, Ms. Sarah Rivas, Mr. Ray Cook, and Ms. Sylvia Salinas for their help during my studies in Texas State University.

I would like to thank my family for their support. Even though I have not seen them for nearly two years, I maybe not able to go further if they are not there.

TABLE OF CONTENTS

Page

LIST OF TABLES

Table **Page**

LIST OF FIGURES

Figure **Page**

ABSTRACT

There has been a growing research interest in pursuing green and low carbon production systems, but only few if any quantitative approaches or systematic tools are available in literature. This research aims to fill this gap by synthesizing onsite renewable energy with the production-inventory model to attain net-zero carbon manufacturing operation. Meanwhile, modern industrial robotics manufacturing process is studied and analyzed to minimize the energy usage. We strive to address two fundamental questions. First, is it economically viable to integrate onsite wind and solar generation into large manufacturing facilities? Second, is it technically feasible to achieve a net-zero energy production-inventory system based on intermittent power? To that end, we synthesize the renewables generation technologies with multi-period, production-inventory system to create a multi-stage optimization model. We optimize the generation capacity, the production quantity, and the stock level in each period such that the aggregate energy and non-energy cost is minimized. Our model is tested in ten different locations with a wide range of wind speed and weather profile. The results show that virtually any manufacturing facility around the world can realize 100 percent renewable energy penetration at an affordable cost.

CHAPTER I

INTRODUCTION

Background

By converting solar energy into living tissue over millions of years ago, plants were buried to produce coal, oil and natural gas, which have been found valuable for manufacturing from them such as textiles, plastics and various kind of petrochemical products. When the use of fossil fuels are burnt, greenhouse gases are released. Industry's use of traditional energy source has been blamed for the contributor of global warming, not to mention human activities of emitting carbon dioxide. Meanwhile, the world population is rising in recent years with the increasing energy use, which requires the increased usage of all kinds of energy. New technology and manufacturing process for renewable energy sources is now or will be an important factor in sustaining the civilization, while providing the necessities of life, especially for renewable energy.

Hazardous chemicals escape in the hydrological cycle through anthropogenic activities. Variant air pollutant from industrial facilities and other activities may cause adverse effects on the environment as shown in Figure 1. Environment PollutionToxic substances are found in the general circulation and deposit to different tissues when human enter and contact with different pollutants via inhalation and ingestion (Kampa et al. 2008). Human health effects can range from respiratory system, cardiovascular system to nervous system. In this case, a total new format of energy source is desirable to be applied to human daily life to reduce the effects because of the

traditional energy source.

Figure 1. Environment Pollution

Taking action unilaterally by claiming that some countries should limit emission levels is not always helpful for controlling the process of global warming. Meanwhile, it is difficult to predict the complex relationship between greenhouse gas and global temperature due to the processes of the climate system since the nature variability transfer heat by winds, currents and hydrological cycle. The link between resource use and productivity need to be re-built for the whole society to take use of scientific and technological know-how in developing a whole new production process.

Three main factors such as environment, resources and pollution are the problems the humanity faces, while the manufacturing industry is one of the main roots of all this kind of environmental pollution mentioned. It is an important topic for manufacturers to minimize the environmental impact of the manufacturing industry. With the increasing need of coal, oil, gas and other non-renewable natural resources,

it is or soon will be feasible to supply all the need of energy from renewable natural source. Those kind of cleaner energy is not only inexhaustible, but also non-polluting that attract attention to the reasonable use of renewable energy.

Most of the energy is utilized now via combustion processes from coal, natural gas and waste which generate greenhouse gases. With the urgent need of protection of natural environment, there has been renewed focus on influence of the green technology and manufacturing. Environmental strategy is moving from being an environmental strategy for environmental and green strategy. Meanwhile, manufacturers can improve the real action of protecting the environment while achieving big economic impact at the same time (Omer et al. 2008 and Deif et al. 2011). Technically, green manufacturing by minimizing negative environmental impacts, conserving energy and resources, is defined as a concrete embodiment of the sustainable development of human society in the modern manufacturing industry, which can be lower raw material gains, increase production efficiency and reduce environmental safety expenses. Two important factors include in the idea of green manufacturing: pollution prevention and product stewardship (Lieberman et al. 1988 and Porter et al. 1995). Pollution prevention reduces the usage of resources and the amount of waste generated. While product stewardship can design products and process with more caution on the surrounding environment, companies are also allowed to use the reputation of “green” to gain competitive advantage (Hart et al. 1995). Currently, conventional energy constitutes 80 percentage of global energy consumption. From Figure 2 and 3, we can see that the world solar and wind energy

has great potential for further usage. More renewable energy should be integrated into manufacturing process to reduce the influence on our planet.

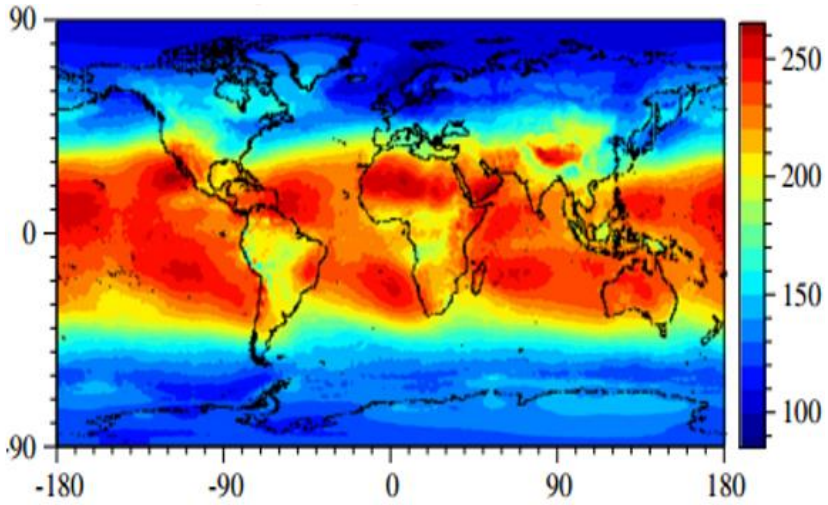

Figure 2. Surface Downward Solar Radiation (W/m^2)

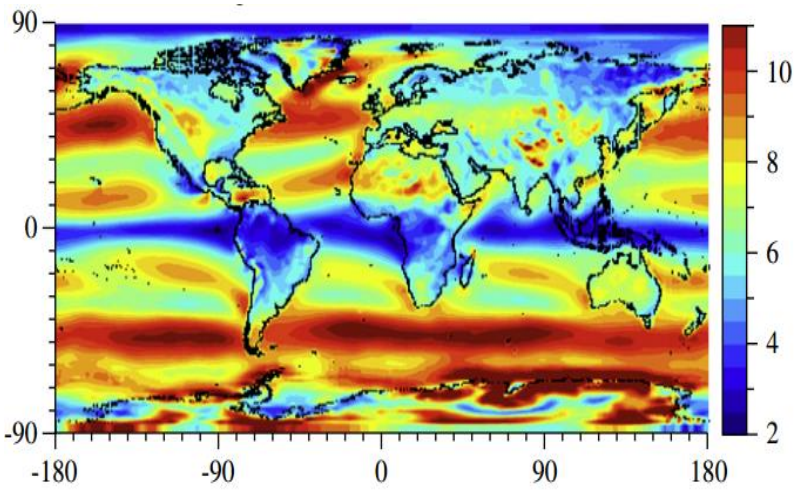

Figure 3. Annual Wind Speed (m/s) on Top of 100 m

Even though much studies can be potential focus: 1) Green manufacturing: reduce material waste and improve the production processes, 2) Cloud computing: extremely high speed and real-time feedback computation capability for manufacturing machines, 3) Big data analysis: provide efficient control method based on remote libraries of object data, trajectories and images, 4) Robotic assembly analysis for automation: enhance the assembly efficiency to decrease energy usage.

Green Manufacturing

Contradict to people's original view on green manufacturing, manufacturers will be paid off by the costs saved in systems using fewer resources and less wastes in the process as well as the product. Green manufacturing also can reduce production cost and obtain more time to improve the production processes by reducing material wastes and energy consumption as shown in Figure 4. Moreover, green manufacturing deals with problems of environmental sustainability by reducing the hazardous emissions, eliminating wasteful resources consumption and recycling, which are examples of sustainable green manufacturing activities (Adams 2001, Darnall et al. 2008 and McDonough et al. 2003).

Figure 4. Advantages of Green Manufacturing

There are still a number of important factors for the manufacturing industry

moving toward to green operation practices. Aware of the significant environmental problems of industrial wastes and emissions, governmental agencies take initiatives toward to the environmental impact control and restoration by making as serious of policies, regulations, and laws, which has achieved significant progress in advancing the environmental performance of industrial production activities (Sawhney et al. 2007). Under the pressure of the laws and policies, the manufacturer is driven to design and implement green manufacturing processes.

With the rapid development of global economic, it requires that manufacturers break the boundaries of administrative regions and organizations, incorporate into the global industrial supply chain. The resources are utilized more effectively if the commercial operations are divided with more proportions. Many advanced manufacturing models and technologies have been proposed. Agile manufacturing is used to understand the commercial environment and become flexible, cost effective and productive with consistent high quality (Sharifi et al. 2001). A networked remote manufacturing system is described for remote operation and monitoring system as an advanced user interface (Mitsuishi and Nagao, 1999). To assess the impact of global manufacturing, a model is set up to show that product, material and key supply chain parameters are three important factors (Kara et al. 2010). Digital manufacturing has been considered to reduce product development times and cost, integrate knowledge, decentralize manufacturing parts and products in different production sites and make manufacturers focus on the core competences (Chryssolouris et al. 2009). Product-service systems enable the machine producers to design the integrated services in an

optimal way to increase the sustainable competitiveness of engineering and plant design (Meier et al. 2010). Grid technology in manufacturing is chosen to be applied to product design, technology integration and resource reallocation and scheduling (Tao et al. 2011). Although all the mentioned methods or models have made great contributions to the development of advanced manufacturing system, how to reduce the production waste, enhance resource utilization, adapt to the external environment change and has sustainable resource supply mechanism are still not effectively solved.

Meanwhile, some new technologies have applied in various fields, such as cloud computing, web service, human interaction systems and so forth. There technologies are able to address the above bottlenecks in next generation manufacturing enterprises.

Cloud Computing

Cloud computing treats everything as a service which can be precisely defined and designed as needed in which cloud providers, enterprise requirements and user expectations are the three key factors (Xu et al. 2012). Computing application distribute among servers which are connected and accessible by Internet. Inspired by cloud computing, manufacturing industry utilized the benefits of cloud computing which supports the areas of IT and new business models to arrange the choice of different operation modes, operation management of the services and embedded access of manufacturing equipment and resources based on exiting Internet-based manufacturing. Its purpose it to realize the full sharing and high utilization, provide on-demand use of manufacturing resources. The National Institute of Standards and

Technology (NIST) offers the following definition for cloud computing (Mell et al. 2011):

"Cloud computing is a model for enabling ubiquitous, convenient, on-demand network access to a shared pool of configurable computing resources (e.g., networks, servers, storage, applications, and services) that can be rapidly provisioned and released with minimal management effort or service provider interaction."

A typical cloud manufacturing service platform requires interaction between three groups: the user, application providers and physical resource providers (Wu et al. 2013). Users who do not have the ability, have the need to manufacture products, or those who have the capabilities but stand to gain the advantage by utilizing cloud manufacturing. Application providers should set up the cloud manufacturing environment and receive user requirement for the real manufacturing industry process. When the data are received and created by the cloud based applications, the physical resource providers, who own and operate manufacturing equipment, automatically begin to make the finalized product according to the user requirements.

Some key technologies are involved in the cloud manufacturing (Ning et al. 2011). Cloud technology utilizes a serious of hardware, software and operation system to enable cloud manufacturing providing service to user. Resource scheduling technology is in control of the distribution and scheduling of capability. To build up a safe, stable and perfect architecture, security technology is also a key factor since the cloud manufacturing platform need to exchange large amount of data. Standardization is included for cloud manufacturing since it is reasonable to treat every cloud's

interface type and certificate management standard, which make the arrangement of physical resource easier.

Cloud manufacturing is a network-based manufacturing platform combing information technology and manufacturing needs. By using cloud computing which makes data, application and resources on Internet dynamic and scalable, manufacturing resource virtualization and service-oriented manufacturing capacity can be further exploited for cloud manufacturing. In the cloud manufacturing environment, cloud computing links the users with needs to resource providers to fulfill the needs while meeting the requirement of cost, quality objectives of users. It is increasingly becoming research hotspots for cloud manufacturing and the way of utilizing cloud computing.

With the development of technology, the Internet is introduced into robotics and automation systems. Many technological evolutions and developmental trends have been made possible due to the ubiquity of Internet, especially cloud computing and personal computer, which influence how robotics and automation are deployed. The Internet and personal computer provider new ways for manufacturers integrate resources and data, and at the same time, lower the cost of production. It is increasingly used by companies for exchanging information with distributed uses through Internet. In reality, much research is still needed to implement this field.

Cloud manufacturing needs every parts to work together to make the best use of the various manufacturing resources. As for the robotics and automation, it is complex because of diversified customer requirement. Meanwhile, an industrial robot

consist of various mechanical and electronic components. During a robotic assembly process, the assembly environment is constantly changing and the dimension and geometry of parts could vary from different batches and different suppliers. These variations will increase the assembly cycle time and lower the manufacturing throughput; moreover, assembly failure rate will arise if the assembly process parameters do not change. Because the assembly processes typically have many stages and different control strategies such as hopping and searching, it is almost impossible to construct a physical model to optimize the process parameters. Sometimes, the whole assembly line has to be stopped in order to tune the process parameters such that the assembly system can adapt to the variations. The process parameters of high precision robotic assembly process have to be tuned in order to deal with part variations and system uncertainties. The changes of structural modifications make tremendous impact on the assembly process for robotics.

The dynamic status of cloud manufacturing process requires robot compete the typical lifecycle of products, such as design, fabrication and assembly. The robotics and automation follows the steps of customer requirement and need. For example, a customer orders robot productions through the Internet. The order is immediately sent to the manufacturing database. According to the information of cloud computing gathered, the manufacturer develops details design and starts to transport different parts to the assembly line with the fastest speed according to carefully arranged schedule. When all the parts and components are received in time, the robots on site begin to assembly the parts together and adjust to the energy stored in the grid as

shown in Figure 5. All of the processes mentioned above are automated process and done by cloud manufacturing.

Efficient management of the resource and organization continues through the production process across the product lifecycles. Information feedback is also extremely important to reduce production time and waste of resources. The manufacturer should be able to monitor and control the production process at any time in case of emergency events. As for cloud manufacturing system itself, it should not only have the ability to quickly start and change working status due to new demands, but also relocate the position and facilities (Carter et al. 2010, Framsyn et al. 2003), which make it easily and quickly reuse manufacturing capacity. When a complete manufacturing process is in process, the manufacturing parts transported to the production site. After completing the tasks, the robots are sent back to home site, or to another location for new operations.

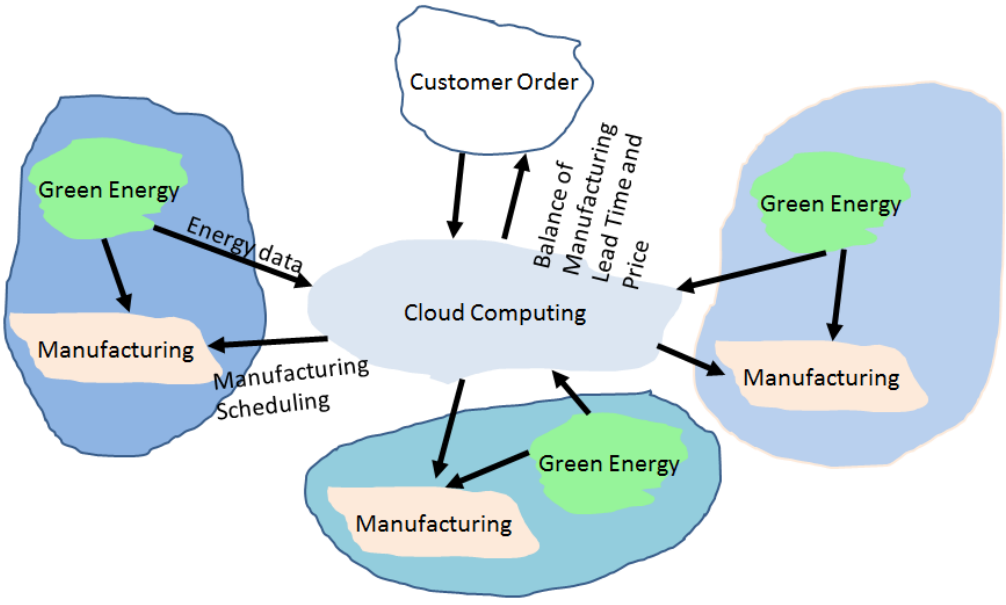

Figure 5. Cloud Manufacturing Process

The interfaces between industrial robots and users is different depending on

the knowledge of the users' knowledge of robots control. Programmers and the robots should understand each other when describing the same concepts. It is easy to program a robot to a specific position. However, robots have to adapt to the new environment based on sensing the information of unknown environment. In other words, the robot should generate its own description, make judges and have the ability to learn. It is necessary to use machine learning for robot to learn the variations via feature abstraction. For the assembly process, it is complex and has so many variations, it is almost impossible to derive a physical model to describe the relation between the assembly process and its process parameters. A viable approach is to identify the model indirectly using the observed system input and output and then explore the system performance using its process parameters.

Big Data Analysis

As advanced analytics technique, big data analysis comprises two aspects: data collection and mining, and how the two combine to create new way of manufacturing. For modern manufacturing, it has numerous sensors, control units, human factors, and power management, etc. Analysis on this kind of huge data will reduce total production cost, increase energy efficiency and mitigate environment impacts. Big data analysis is a new trend of research both in industry and academia. We can make better predictions and smarter decisions to change traditional ideas about the value of experience, and the practice of management. Based on data-driven decisions, it is helpful for manufacturing automation and facilities management. Once the machine control units move to cloud, the method of manufacturing is totally changed. With

machines' head in the cloud, workers could track not only what the status is, but also where the malfunctions take place; how to distribute the assembly line; how to calculate the order; and how to involve humans to work with machines.

Renewable Energy for Manufacturing

With the increasing demand for energy, the electric grid is confronting a grand challenge in keeping the pace with the economic growth. Power grid is affected and changed with time by the loads, customers' need and so on. Electricity still cannot be effectively stored in bulk form. Once generated, it must be distributed and used immediately. Manufacturing industries are a part of large electricity users. While meeting the growing need of manufacturing process, utilities have to shed the peak loads and balance electricity use against the large variations across the year.

Renewable energy is involved with natural phenomena such as wind, sunlight and geothermal heat, as the International Energy Agency defines by Party Irew (2002):

"Renewable energy is derived from natural processes that are replenished constantly. In its various forms, it derives directly from the sun, or from heat generated deep within the earth. Included in the definition is electricity and heat generated from solar, wind, ocean, hydropower, biomass, geothermal resources, and biofuels and hydrogen derived from renewable resources."

Renewable energy replaces conventional fuels like coal and oil and makes up of 15% global final energy consumptions (Lund 2007). There is no doubt that the market will be large, but facing the challenge of lowering the cost and being more convenient, sustained growth is still needed. Wind turbines have become cheaper,

more efficient and reliable and lower investment risk with matured industry. As for e solar energy power markets, the total capacity is still smaller than that of wind power market. Meanwhile, the efficiency of converting solar energy to electricity is still low and it requires policy support to overcome all the shortcomings (Gross et al. 2003). Wave and tidal stream energy devices installed worldwide are mainly for demonstration projects. The overall cost reduction potential of biomass combustion technology are to commercialize high efficiency generating plants and to secure sustainable supplies of relatively low cost fuels.

Robotic Automation for Assembly

With new energy saving technologies applied in industrial manufacturing, energy efficiency is greatly increased per unit price of energy services. However, energy consumption in the medium to long term still decreases for modern industrial manufacturing process. As shown in Figure 6, a modern assembly line involves many industrial robotics. Traditionally, these robots are specially programmed and repeated with the same assembly/welding parameters. However, once the assembly environment changes and parts variation exceeds the expectation, the whole assembly line has to be stopped for adjusting the parameters of certain robots. It takes time and wastes electric energy. In this case, a more advanced manufacturing process has to be developed to further improve the process so as to increase energy efficiency.

Figure 6. Assembly Line (The New York Times 2012)

A high precision robotic assembly process requires a robot to perform assemblies in which the assembly clearance is better than the repeatability of robot. Figure shows the steps about how the industrial robot performs the assembly process. A searching method is used to find the exact position of the work piece. After the part is engaged with the work piece, it is inserted into the work piece using a certain insertion force. During insertion, the tool orientation will change according to the orientation of the work piece to avoid jam. Several parameters need to be tuned in the assembly process, such as search force, search speed, search radius and insertion force. The assembly process performance will degrade if these parameters are not adjusted correctly to adapt to the variations.

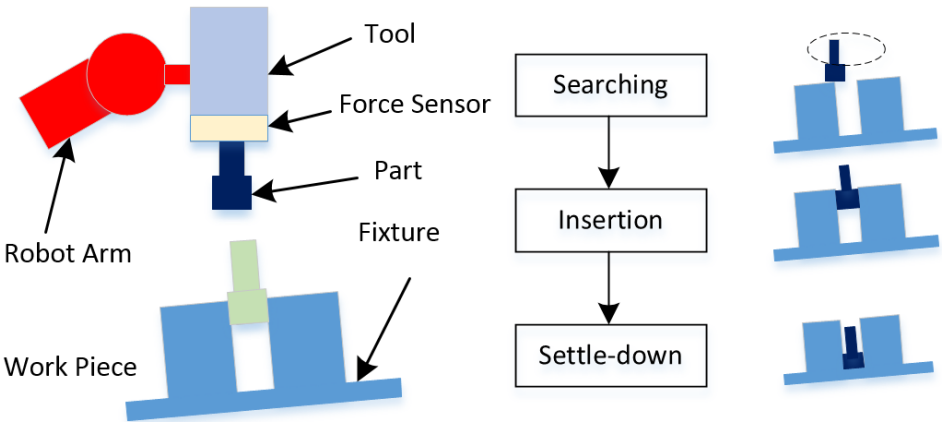

Figure 7. A Robotic System to Perform a High Precision Peg-In-Hole Assembly Process

Typically, the parts could be manufactured in different batches and by different suppliers. Hence the clearance, geometry and dimension of the parts could be different which will increase assembly cycle time and cause assembly failure. To deal with these variations, the process parameters have to be optimized. Therefore, the relationship between an assembly process and its process parameters has to be explored. As we can see, if one of these robots stops working due to system malfunctions and configuration mistakes, the whole system has to stop and need a professional engineer to tune the robot and put it back to work. If robots' heads in the cloud, it would be much easier for workers to discover glitches of robot condition and utilize modern automated control system to fix the problem before any damages happen. Just as James Kuffner at Google in 2010 summarized and concluded: "No robot is an island".

Origination of Thesis

Even though many research efforts have been done, few has relation with renewable energy, not to mention how to integrate product inventory system under intermittent power. This research aims to assist manufacturing firms in designing an

onsite generation system to achieve net-zero carbon environmental performance at minimum cost. We propose a grid-connected DG system consisting of WT, solar PV, and substation to achieve three objectives: 1) minimizing levelized cost of energy, 2) realizing net-zero carbon emission, and 3) facilitating the execution of demand responses. We tackle this design problem in three steps. First, a stochastic programming model is formulated to minimize the DG costs subject to the GEC requirement. Second, we propose a simulation-based optimization algorithm to search for the optimal sizing of WT and PV units considering uncertain load. Third, we design an automated online learning process to decrease machine idle time and increase energy usage efficiency. Lastly, the proposed DG system is tested in ten different cities of the world under a wide range of wind speeds and weather conditions. To test our theory, we built a prototype in the lab setting. Further description will be analyzed in the experimental parts.

CHAPTER II

LITERATURE REVIEW

Renewable Energy for Industrial Applications

Driven by a growing world population, energy use has become a critical concern in the last decades. As one of the cleanest energy, solar energy is abundant, and its use does not add to global warming. It does not have emissions of greenhouse and toxic gasses, does not increase the transmission lines from electricity grids. On the contrary, it increase regional/national energy independence, diversify generation portfolio, enhance the security of energy supply, and accelerates of rural electrification in developing countries. Usually, PV systems convert energy in the photons of sunlight into electricity into two groups: stand alone and grid connected systems. Grid connected systems are systems connected with utility grid. When there is not enough energy from the solar panels, the manufacturing facility will import the energy from the public grid. If more energy is generated by the PV systems, the energy will be feed into the public grid. On the other hand, standalone systems are the systems which are only connected to the manufacturing facility's grid to power the working stations (Libo et al. 2007, Joung et al. 2006). Many remote and isolated industrial applications use solar electricity for a long time such like traffic lights, most of which are standalone systems. Telecommunication industries use storage battery powered by solar energy to assure the continuity of the system. They also apply solar electricity to reduce peak temperature in un-insulated outdoor cabinets which contains telephone equipment. Water desalination industries utilize solar energy to desalinate sea water,

which is economically and technically more competitive than conventional diesel engine powered reverse osmosis alternatives. Apple Inc. works with local partners to develop renewable energy to power the data centers for the good of the planet.

Studies have been proposed to implement green manufacturing issues on technical and managerial. Circular supply chain served as a management code of green manufacturing generated and took environmental, economic and social benefits into consideration (Du et al. 2010). Different factors involved in the green manufacturing process have been conducted to be under control for supply chain, indicating that material, process, packaging, working environment and waste system are the main factors that have direct influence on green manufacturing (Udomleartprasert et al. 2004). A multi attribute model called Performance Value Analysis is presented to overcome the intangible benefits which offers better advantages over the non-green manufacturing system (Sangwan 2006), etc. These successful studies promotes the development of green manufacturing

To reduce the power demand during the peak periods. “Just-for-Peak” buffer inventory is set up during peak period without sacrificing system throughput for manufacturing systems (Fernandez et al. 2013). A model is build up for load management in process industries to determine the industry response (Ashok 2006). The Time-of-Use (TOU) based electricity demand response problems is proposed to minimize the total electricity consumption and cost by shifting use according to the status of power grid. However, all of the methods mentioned above do not concern the fact of integration of renewable energy.

Even though technologies have experienced the most rapid development, it is obvious of two main challenges of renewable energy. One is how to integrate the electricity generated of renewable energy into existing energy system (Lund 2006). The other is about the transportation of the energy. Moreover, since the population of the world is increasing, which motivates the people to increase the utilization of renewable energy. Fossil fuels should be controlled and managed, and renewable energy need to ready to play a role for the industrial applications. Some energy policies like Feed-in tariff , renewable portfolio standard and incentives are implemented by many countries around the world (Solangi et al. 2011) including tax exemption, subsidies, formation incentives and others.

Sustainable manufacturing operations have been discussed in literature, including energy conservation, dynamic electricity pricing and renewable energy integration. Though all these methods strive to improve the economic or the environmental performance, their approaches to manufacturing sustainability are quite different. In this section we revisit the modeling techniques and the design methods for green manufacturing systems. For strategic discussions on green manufacturing and sustainable operations, readers are referred to the studies (Kleindorfer et al. 2005)

The idea of energy conservation is to increase the machine efficiency or reduce the tool idle time so that less electricity is consumed during the production. Mouzon et al. (2007) minimize the energy consumption and the total completion time by controlling the on and off of underutilized machines. Considering an aggregate production environment, Choi et al. (2014) develop a linear programing model to

minimize a weighted objective function comprised of energy use, inventory holding and backorder costs subject to resource constraints. Lin et al. (2013) use a Markov decision model to minimize the energy consumption in a multi-machine, multi-buffer production environment by shortening machines' idle time. Chen et al. (2013) minimize the energy consumption of a serial assembly line through effective scheduling of machine startup and shutdown procedures. Though in nearly every industrial enterprise, there are many profitable energy conservation opportunities, the hindrance to reaping the potential benefits is the lack of an internal management framework in which to find, value, and execute these projects. Besides, energy conservation alone cannot achieve superior environmental performance (e.g. zero carbon emissions) unless external renewable energy sources are injected into the manufacturing process.

The third research line advocates the integration of renewable energy into the manufacturing facilities through onsite or distributed generation scheme. Taboada et al. (2012) propose an onsite, grid-tied PV system to power a 15-MW wafer fab in conjunction with a substation. Up to 10,000 tons of carbons could be avoided when the PV capacity reaches one-third of the mean load based on five U.S. fab facilities through numerical experiments. By incorporating solar PV and WT to power a large industrial facility, S. Villarreal et al. (2013) expand the onsite renewable energy portfolio. The results show that if the local wind speed is above 4.8 m/s and the yearly overcast days are less than 35%, onsite generation becomes cost-effective. By taking into account the onsite renewable power as well as energy storage, Moon et al. (2014)

optimize a multi-process, multi-machine manufacturing scheduling problem. These researches show that it is possible to lower the carbon footprint of manufacturing processes. In this research, we take one step further to power a net-zero carbon production facility bound by uncertain load curtailments under demand response contract.

High Precision Robotic Assembly

In a modern manufacturing process, the changes in assembly environment, the variability of dimensions and geometries of the parts, and other uncertain variables generate unpredictable location errors which make conventional position-based tactics unsuccessful. Both assembly failure rate and cycle time will increase if the process parameters are not adjusted accordingly against the variations. Sometimes a whole assembly station has to be stopped for days in order to tune several key process parameters. For assembly processes requiring high precision and tight tolerance criteria, an automatic parameters optimization algorithm or online high precision robotic assembly process is essential as it mitigates the variation effect, assures assembly performance and lowers the production cost.

In traditional robotic assembly application, the passive compliance device or the Remote Center Compliance has been utilized to reduce the contact force, to prevent tools and parts from being damaged, and to compensate for vibration, clearance and positioning errors due to machine inaccuracy (Meyer et al. 2006). However, passive compliance devices need to be specifically designed and tailored for parts with different dimensions and geometries.

For high precision robotic assembly process, robotic assembly parameter optimization based on force control technology has received much attention both in the industry and the academic communities. Robotic assembly using force control is able to shorten the cycle time, reduce the contact force, and lower the risk of jamming, wedging and galling (Brogardh, 2007). In addition, the requirements on the accuracy of fixtures and grippers can be significantly relaxed (Ostring, 2002). However, the force control method requires extra supports such as software package and force sensor, which cause the robot control system more complex and expensive.

Several methods have been proposed to optimize the assembly parameters. Logic-branching is proposed to find the optimum solutions of the states after the system is initialized (Vaaler et al. 1991). As a model-free algorithm, genetic algorithm (GA) is applied to randomly search for the optimal or near optimal assembly process parameters (Marvel et al. 2009). Artificial Neural Network (ANN) is adopted to improve the performance of assembly parameter optimization without conducting any experiment (Marvel et al. 2011). Design of Experiment (DOE) based method offers a systematic approach to optimizing the assembly process parameters (Zhang et al. 2011). After 2430 experiments are performed for one optimization iteration, the most sensitive parameters are identified and properly tuned to ensure the adaption to the environmental changes. Even though these aforementioned methods are quite promising in optimizing the process parameters, it is rather challenging to implement these methods in real-world applications because of the low efficiency, high cost and long computing time.

For online robotic parameter optimization process involved with many assembly stages such as cylindrical, radial and multi-stage insertions, it is impossible to construct a physical model. Some off-line optimization algorithms like DOE search for global optimal parameters for complex assembly process based on existing experimental results. A model-driven algorithm is more preferable in terms of improving the parameter optimization efficiency by finding the optimal assembly process parameters online.

In this research, a support vector regression (SVR) enabled algorithm is proposed to solve the online parameter optimization problem without stopping the assembly station. A typical peg-in-hole assembly process is used to demonstrate the performance of the proposed algorithm in a laboratory setting. Compared with the traditional methods, both the efficiency and accuracy are significantly improved based on the SVR enabled algorithm.

Production-Inventory Systems Studies

To design production-inventory systems considering elastic electricity pricing or demand response contracts. Ierapetritou et al. (2002) construct a two-stage stochastic programming model to plant operation modes, optimize the production rate, and inventory level for an air separation company subject to real-time electricity rate. Mitra et al. (2012) develop a deterministic formulation which is able to efficiently handle the transient plant behavior by considering the seasonality of electricity tariffs. Karwan et al. (2007) solve a similar problem using simulation-based optimization through a rolling horizon method. Fernandez et al. (2013) propose to pro-actively

build work-in-process units to avoid the power usage during the periods of peak electricity prices Instead of using stochastic models. By minimizing time-of-use electricity cost under pre-determined production rates, Wang et al. (2013) adopt a systems approach to production scheduling. Chao et al. (2008) determine the optimal production policy for a single-machine manufacturing system when random load curtailments take place under demand response contract. In this thesis, we incorporates the demand response program into the design and operation of the DG system to fill the energy shortage resulted from load curtailment requests.

Production-inventory models under uncertainties have been extensively investigated in operations management literature Yano et al. (1995) and Mula et al. (2006). Federgruen et al. (1984) design a scholastic centralized production-inventory program that fulfills the random demands from several locations by minimizing the expected holding and backorder costs. (Lee, 1988) develop a back-track dynamic programing method to find the optimality of a serial production system that minimizes operating, holding, and backorder costs subject to random yield. Kira et al. (1997) propose a hierarchical method to optimize a multi-period, multi-product production scheduling problem under a finite set of demands based on stochastic linear programming. More recently, Higle et al. (2011) propose a stochastic optimization model to schedule the production operation considering both supply and demand uncertainty via Markov decision process. Extant product-inventory models are shown to be effective in dealing with uncertainties arising from demand, production, yield, and supply. To lower the environmental impacts, it is imperative to incorporate the

renewable energy into the production-inventory decision to achieve the superior environmental performance.

CHAPTER III

COST ANALYSIS OF ONSITE GENERATION SYSTEM

We design an onsite DG system consisting of multiple distributed energy resources (DER), namely WT units, solar PV, to power a large manufacturing facility. These DER units function as the primary energy sources, and the substation mitigates the uncertainty of renewable energy generation by WT units and solar PV. The energy gap is intended to be filled by drawing the electricity from the power grid if the aggregate power of the DG is below the demand of the manufacturing enterprise. On the other hand, if the DG system produces surplus solar electricity, it can be fed into the main utility grid via net metering or feed-in tariff scheme. As return, the customer is able to generate energy revenue by selling the net metering energy back to the utility grid.

Onsite Wind and Solar Generation System

We choose WT and solar PV as the DER units to construct the onsite DG system to power manufacturing facility because of the technical maturity and scalability shown in Figure 8. Since the power output of WT and PV is intermittent, energy reliability plays the key role in designing and operating the DG system. The risk of energy shortage can be mitigated by increasing the generation capacities of WT and PV. However, this is not a practical approach as it requires huge upfront capital investments.

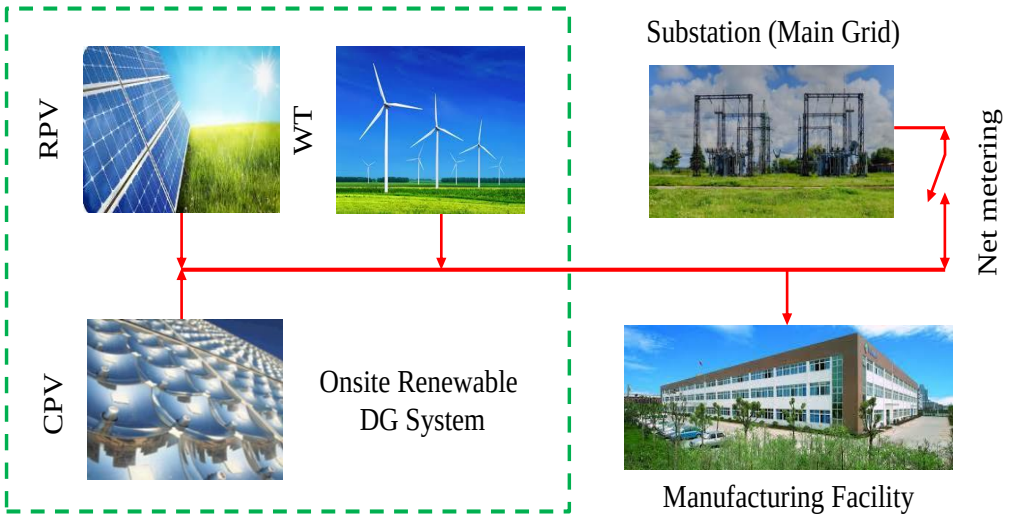

Figure 8. A Grid-Connected Distributed Generation System (Li et al. 2015)

A trade-off must be seriously considered between the capacity cost and the risk of power shortage. Given all the situation, the following components mainly constitute the lifecycle cost of a DG system: carbon credits or subsidies, initial capital, operation and maintenance (O&M), utility bills, and net metering revenue. Indeed the last two components, utility bills and net metering revenue, are the incomes for the manufacturer. It is either because of the renewable energy incentives provided by governments or utility companies saved due to renewable energy. Therefore, we perform a detailed analysis on different cost components below. Unless specified, the unit for power is megawatt (MW), and the unit for energy is megawatt-hour (MWh).

Load Profile of Industrial Facilities

In this research, we take the electricity load of a wafer fab as an example to characterize the energy usage of semiconductor manufacturers. The results can be extended to other industries such as automobile manufacturing, chemical and oil refinery, plastic, and cloud computing and data centers. It is worth mentioning that the load profile of wafer fab differs from residential consumers because a manufacturing

facility typically runs in 24/7 mode. Energy consumption comprised of 12-month data is obtained from our industry partner in Texas, USA. The electricity demand curve is depicted for a period of 12 months from January to December in 2010 in Figure 9. The actual data value has been normalized for privacy, yet the seasonality and the monthly dissimilarity are preserved.

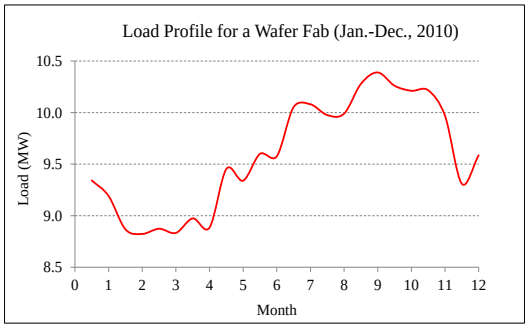

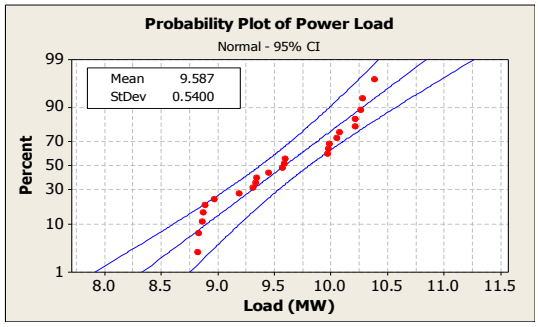

Figure 9. Wafer Fab Load Profile **Figure 10. Normality Test**

(Pictures originally from Li et al. 2015)

The load profile shows that there exists a strong cyclical pattern coupled with short-term variations. The eletricity demand between later January and early April is about the lowest around 8.8 MW. It ramps up from April and reaches the highest point at 10.4 MW in September before decreasing to 9.3 MW in later November. The load profile indicates that the time between June and October is the busiest season because the facility is running in full scale in order to meet the customer demand. Figure 10 shows the results of the probability test on the annual load data which indicates that the hourly demand can fit a normal distribution with mean of 9.587 MW and standard deviation of 0.54 MW at 95% confidence level.

Two design strategies are often used to handle the load variability for planning a DG system: the worst-case design and the distribution-based design. In worst-case

design, the peak load is used to control the generation capacity such that the hourly demand and the environmental criteria are satisfied. The design based on the worst-case scenario is relatively straightforward, while it may result in over investment. In distribution-based design, seasonal or temporal load variations are decomposed into a set of probability functions in daily, weekly or monthly basis. Then the seasonality behavior is translated into a chance constraint in which the probability that the power is less than the load is controlled by the so-called loss-of-load probability criterion. It is worth emphasizing that the performance of a grid-connected DG system is usually measured by its long-term energy yield. Transient load variation is not the main concerns as short-term energy gap can be filled by drawing the electricity from the main grid.

The distribution-based design avoids overinvestment in capacity while maintaining the necessary level of energy reliability. In this research, we adopt this kind of design approach by decomposing the load variation into multiple normal distribution functions in monthly basis. We compute the mean and the standard deviation (Stdev) of the facility load based on the 12-month data in Figure 8, and the results are summarized in Table 1.

Table 1. Mean and Standard Deviation of Monthly Power Load

Month	January	February	March	April	May	June
Mean (MW)	9.267	8.846	8.853	8.930	9.397	9.588
Stdev (MW)	0.232	0.221	0.221	0.223	0.235	0.240
Month	July	August	September	October	November	December
Mean (MW)	10.068	9.983	10.334	10.237	10.093	9.448
Stdev (MW)	0.252	0.250	0.258	0.256	0.252	0.236

Installation, Maintenance and Carbon Credits

Installation cost represents the major of upfront DG investment. Let $\mathbf{P}^c=[P_1^c, P_2^c,\ldots, P_g^c]$ be the power capacity of generation type i for i=1, 2, …, g. For example, P_1^c and P_2^c could be the capacity of WT generators and PV panels, respectively. Then the annualized DG installation cost can be estimated as:

$$C_{in} = \frac{r(1+r)^n}{(1+r)^n - 1}\sum_{i=1}^{g} a_i P_i^c = \phi(n,r)\sum_{i=1}^{g} a_i P_i^c \,, \qquad (1)$$

where a_i is the capacity cost per MW for generating type i. Note that $\phi(n,r) = [r(1+r)^n]/[(1+r)^n - 1]$ is the capital recovery factor where n is the number of years of paying off the loan, and r is the annual interest rate.

Although the resources of wind and solar generation are free, the O&M cost has to do with two things: 1) leasing the land to lay up WT, PV, and other accessory equipment; and 2) the maintenance and the repair of WT and PV because of system degradation and failures. We use P_{it} be the actual power output of generation type i at hour t. The annual O&M cost of the DG system can be estimated as:

$$C_{om} = \sum_{t=1}^{h}\sum_{i=1}^{g} b_i P_{it} \,, \qquad (2)$$

where b_i is the O&M cost per MWh of generation type i, and h is the calendar hours in a year with h=8,760 hours. It is worth stating that the meaning of the value P_{it} differs from P_i^c in that the former is the instantaneous power which changes over time, while the latter is the generation capacity which is a fixed value.

Various incentive programs have been proposed by governments around the world to motivate the investment and adoption of wind and solar energy. Carbon

credits and equipment subsidies are among the most popular incentive schemes. Equipment subsidies can be treated as one-time cost saving to renewable energy investor. The amount of carbon credits rely on the actual renewable energy generated. Let C_{cr} be the total carbon credits received by the manufacturer in one year:

$$C_{cr} = \sum_{t=1}^{h} \sum_{i=1}^{g} c_i P_{it} , \tag{3}$$

where c_i represents the carbon credits per MWh for generation type i. Equation (3) is quite general in the sense that if the incentive program for energy type i expires, we simply set c_i=0; on the other hand, if c_i<0, it means a penalty cost is imposed on generation technology i due to the emission of greenhouse gases, such as fossil fuel based generators.

Annual Production Loss

Typically, large manufacturing enterprises sign a specific demand response (DR) contract with the local utility company. They agreed to curtail the load during the peak hours for residential users. In return, the manufacturer is able to enjoy a reduced electricity fee or receive a lump-sum payment (Baldick et al. 2006). In this research, we mainly focus on the interruptible/curtailable demand response program since it is widely agreed by manufacturing industries. The manufacturer has to turn off some machines to meet the load reduction level when a contingency call is received. Let C_{dr} be the annual production losses incurred in all contingent events, then

$$C_{dr} = \varepsilon \sum_{t=1}^{h} \{L_t\}^+ , \tag{4}$$

where L_t is the load reduction level in MW at time t. Here $\{L_t\}^+=L_t$ if $L_t>0$, or $\{L_t\}^+=0$ if $L_t=0$. Note that ε is the production loss per MWh curtailment ($/MWh).

Annual Utility Cost

A large portion of electricity bills paid to the utility company, are saved as a result of adopting onsite DG system. However, it is still necessary to draw the electricity from the main grid when the load exceeds the DG output. By considering DR events and DG output, the annual utility cost can be estimated as

$$C_{bill} = \rho \sum_{t=1}^{h} \left\{ D_t - \{L_t\}^+ - \sum_{i=1}^{g} P_{it} \right\}^+ , \tag{5}$$

note that ρ is the discounted utility price ($/MWh) due to the DR participation, and D_t is the facility's electricity demand in time t.

Feed-in Tariffs

The produced and injected solar energy into the grid has the same economic value of the energy sold to the customers. Feed-in Tariffs were a protocol for the exchange of the electric energy generated. Feed-in Tariffs permit the manufacturer to return surplus renewable energy to the main utility grid when the DG output exceeds the load requirement. This specific situation occurs when the wind blows hard, the solar radiation is strong, or the facility enters the low production season. The annual income from the feed-in Tariffs can be estimated as

$$C_{nm} = \delta \sum_{t=1}^{h} \left\{ \sum_{i=1}^{g} P_{it} + \{L_t\}^+ - D_t \right\}^+ , \tag{6}$$

Where δ is the revenue rate ($/MWh) each time one MWh electricity is fed into the electricity grid. In net metering, the meter's reading increases when electricity

is drawn from the grid, and decreases if renewable energy is fed into the grid. Hence we have $\delta=\rho$.

Interruptible/Curtailable Demand Response

Interruptable/curtailable demand response (I/C DR) program is the most widely used load curtailment contract in manufacturing industry. Customers agree to curtail the load upon request in exchange of the monetary reward or a discounted electricity rate. In a pay-as-you-go scheme, the utility company pays a penalty to the customer for each contingency call. In a pay-in-advance scheme, the utility offers a discounted electricity price to the participants during the contract period. This research assumes the manufacturer accepts the pay-in-advance policy and is willing to curtail the load upon request.

The maximum and the minimum curtailment duration, denoted as $T_{\max}$ and $T_{\min}$ respectively, usually are written in the contract. In general, we have $1 \le T_{\min} \le T_{\max} \le 8$ hours for a typical I&C DR program (Aalami et al. 2010). However, the manufacturer does not have the advance knowledge about the curtailment duration until being called. Let T be the random duration of a curtailment event, and τ be its realization. T can be treated as a uniform random variable with the following probability density function:

$$f_T(\tau) = \begin{cases} \dfrac{1}{T_{\max} - T_{\min}}, & T_{\min} \le \tau \le T_{\max} \\ 0, & otherwise \end{cases} \tag{7}$$

The curtailment level may differ in each contingency call, yet the maximum amount of reduction usually does not exceed 20 percent of the facility's mean load

(Aalami et al. 2010). We use the discrete probability model to characterize the variation of curtailment levels. Let l_j for j=1, 2, …, q represent the actual realization of curtailment levels, and $l_1<l_2<\cdots<l_q$. The probability mass function can be expressed

$$\Pr\{L_t = l_j\} = p_j, \qquad \text{for } j=1, 2, \ldots, q \tag{8}$$

where L_t is the random variable representing the load curtailment level in time t. Obviously, the sum of p_j for all j should be equal to unity.

Though the total curtailments usually does not exceed ten times a year, the actual start time of a curtailment is not known to the manufacturer until being called 30-60 minutes in advance. Let N be the number of curtailment during the course of a year. The occurrence of I/C DR events can be modeled as a Poisson process as follows

$$\Pr\{N = n\} = \frac{(\lambda t)^n e^{-\lambda t}}{n!}, \qquad \text{for } n=0, 1, 2, \ldots \tag{9}$$

where λ is the curtailment request rate. For instance, if the average curtailments in a year is five, then λ=5 calls/year. Based the value of λ, we can simulate the number of DR events and the start time of each event. The curtailment level usually does not exceed 20% of the factory's nominal load, and the average duration of a curtailment is eight hours.

Annualized Cost for DG System

By aggregating the cost components in equations (1)-(5) and (7), the annualized cost of the DG system is given as follows

$$\begin{aligned} C_{DG}(\mathrm{P}^c) = {} & \xi(T,\theta)\sum_{i=1}^{g} a_i P_i^c + \sum_{t=1}^{h}\sum_{i=1}^{g}(b_i - c_i)P_{it} + \varepsilon\sum_{t=1}^{h} I(L_t)L_t \\ & + \sum_{t=1}^{h}\left[\left(\rho I(Y_t) + qI(-Y_t)\right)\left(D_t - I(L_t)L_t - \sum_{i=1}^{g} P_{it}\right)\right] \end{aligned} \tag{10}$$

With

$$D_t = \frac{1}{\tau}\sum_{j=1}^{m} e_{j\lceil t/\tau \rceil} x_{j\lceil t/\tau \rceil}, \quad \text{for } t=1, 2, \ldots, h \tag{11}$$

In equation (9), τ is the length (or the number of hours) of each production period, e_j is the energy consumed in making one unit of product j for j=1,2, …, m, and x_j is the amount of product j produced during τ. Here $\lceil \bullet \rceil$ is the operator that takes the smallest upper integer of the non-negative value. For instance, if t/τ=4.3, then $\lceil t/\tau \rceil$ is qual to 5.

Production-Inventory Model with Net-Zero Carbon Emission

The main concerns with the adoption of onsite DG system include the upfront investment and the power intermittency. To deal with such problems, we propose a renewables-based, multi-period, production-inventory planning model to explore the technological and financial feasibility. The model aims to achieve two objectives: 1) minimizing the overall production cost comprised of energy and non-energy expenses; and 2) realizing net-zero carbon manufacturing operation goal by attaining the 100 percent GEC target. Such production-inventory decision, denoted as Problem P1, can be formulated as a mixed integer stochastic programming model as follows:

Problem P1:

Minimize:

$$f(\mathbf{x},\mathbf{y},\mathbf{z},\mathbf{P}^c) = \sum_{j=1}^{m}\sum_{k=1}^{n} c_{jk}x_{jk} + \sum_{j=1}^{m}\sum_{k=0}^{n} h_{jk}y_{jk} + \sum_{j=1}^{m}\sum_{k=1}^{n-1} b_{jk}z_{jk} + C_{DG}(\mathbf{x},\mathbf{P}^c), \tag{12}$$

Subject to:

$$x_{jk} - y_{jk} + z_{jk} \geq d_{jk}, \qquad \text{for all } j \text{ and } k=1 \tag{13}$$

$$x_{jk} + y_{j,k-1} - y_{j,k} - z_{j,k-1} + z_{jk} \geq d_{jk}, \quad \text{for all } j \text{ and } k\geq 1 \tag{14}$$

$$\sum_{j=1}^{m} r_{js} x_{jk} \le w_{sk}, \qquad \text{for given } s, \text{ and } k \tag{15}$$

$$\Pr\left\{\sum_{i=1}^{g} P_{it} + P_G \ge D_t\right\} > 1-\gamma, \qquad \text{for } t=1, 2, \ldots, h. \tag{16}$$

$$\sum_{t=1}^{h}\left(D_t - (I(L_t)L_t) - \sum_{i=1}^{g} P_{it}\right) \le 0, \tag{17}$$

x_{jk}, y_{jk}, z_{jk} are non-negative integers, and P_1^c, P_2^c, …, $P_g^c \ge 0$. (18)

Problem P1 is a stochastic programming model owing to the random wind and solar power. Note that x_{jk}, y_{jk}, and z_{jk} are integer decision variables on behalf of the production quantity, inventory level and backorders of product j in period k, respectively. In addition, P_i^c is the decision variable acting as the power capacity of generation technology i. The objective function (12) is to minimize the annual production cost comprised of energy and non-energy expenses. In particular, the first three summations are the standard costs of production, inventory holding, and backorders. Here c_{jk}, h_{jk}, and b_{jk}, respectively, represents the unit cost of material/labor, holding, and backorder of product j in period k. The term $C_{DG}(\mathbf{x}, \mathbf{P}^c)$ is the energy cost given in equation (10). Constraints (13) and (14) are the basic production-demand balance equations where d_{jk} represents the demand of product j in period k. Constraint (15) defines the capacity limits of the facility, where r_{js} is the amount of resource s for producing one unit of product j, and w_{sk} is the total available capacity for s in period k. Constraint (16) is the chance constraint stipulating the loss-of-load probability (LOLP) criterion of the DG system. Note that γ is the acceptable LOLP, and P_G is the main grid power. To meet the net-zero carbon emission, constraint (17) states that the electricity consumption in a year should not exceed the

total renewables generation from the DG system.

Translation into a Three-Stage Decision Model

In fact, Problem P1 is a mixed inter stochastic programming model, and this type of problem in general is difficult to solve. Below we propose a three-stage optimization strategy to search for the optimal **x**, **y**, **z**, and $\mathbf{P}^c$. The overall cost is the sum of $f_2(\mathbf{x}, \mathbf{y}, \mathbf{z})$ in stage 2 and $f_3(\mathbf{P}^c; \mathbf{x})$ in stage 3.

Problem P2-1:

$$\text{Minimize: } f_1(\mathbf{x},\mathbf{y},\mathbf{z}) = \sum_{j=1}^{m}\sum_{k=1}^{n} c_{jk}x_{jk} + \sum_{j=1}^{m}\sum_{k=0}^{n} h_{jk}y_{jk} + \sum_{j=1}^{m}\sum_{k=1}^{n-1} b_{jk}z_{jk} \tag{19}$$

Subject to:

$$x_{jk} - y_{jk} + z_{jk} \geq d_{jk}, \quad \text{for all j and } k=1 \tag{20}$$

$$x_{jk} + y_{j,k-1} - y_{j,k} - z_{j,k-1} + z_{jk} \geq d_{jk}, \quad \text{for all j and } k\geq 1 \tag{21}$$

$$\sum_{j=1}^{m} r_{js}x_{jk} \leq w_{sk}, \quad \text{for given } s, \text{ and } k. \tag{22}$$

$$x_{jk}, y_{jk}, z_{jk} \text{ are non-negative integers.} \tag{23}$$

Problem P2-2:

$$\text{Minimize: } f_2(\mathbf{x},\mathbf{y},\mathbf{z}) = \sum_{j=1}^{m}\sum_{k=1}^{n} c_{jk}x_{jk} + \sum_{j=1}^{m}\sum_{k=0}^{n} h_{jk}y_{jk} + \sum_{j=1}^{m}\sum_{k=1}^{n-1} b_{jk}z_{jk} \tag{24}$$

Subject to

$$\frac{1}{\tau}\sum_{j=1}^{m} e_{j\lceil t/\tau \rceil}x_{j\lceil t/\tau \rceil} \leq I(L_t)(D_t - L_t) + [1 - I(L_t)]P_G, \quad \text{for } t=1, 2, \ldots, h \tag{25}$$

Other constraints are the same as P2-1.

Problem P2-3:

Min:

$$f_3(\mathrm{P}^c;\mathrm{x}) = \xi(T,\theta)\sum_{i=1}^{g} a_i P_i^c + \sum_{t=1}^{h}\sum_{i=1}^{g}(b_i - c_i)P_{it} + \varepsilon\sum_{t=1}^{h} I(L_t)L_t + \sum_{t=1}^{h}\left[\left(\rho I(Y_t) + qI(-Y_t)\right)\left(D_t - I(L_t)L_t - \sum_{i=1}^{g} P_{it}\right)\right] \tag{26}$$

Subject to:

$$\Pr\left\{\sum_{i=1}^{g} P_{it} + P_G \geq D_t\right\} > 1-\gamma, \qquad \text{for } t=1, 2, \ldots, h \tag{27}$$

$$\sum_{t=1}^{h}\left(\sum_{i=1}^{g} P_{it} - D_t - I(L_t)L_t\right) \leq 0, \tag{28}$$

$$P_1^{\mathrm{c}}, P_2^{\mathrm{c}}, \ldots, P_g^{\mathrm{c}} \geq 0. \tag{29}$$

For the above three stages problems, we are intend to solve each stage step by step. In stage 1, assuming electricity provided is abundant; we optimize the production quantity, the stock level, and the backorders to minimize the non-energy cost of the production system. In stage 2, the demand response events are inserted into the solution obtained from Stage 1, and re-solve the production-inventory model by integrating the load curtailment constraint. This constraint captures two scenarios: if DR occurs at t, the total power load is confined to D_t-L_t. If there is no DR, the load could be as $+\infty$ denoted as grid P_G. Note that D_t is the power consumption without load curtailments.In stage 3, we recomputed D_t based on the new solution from Stage 2, and minimize the energy cost by optimizing the capacity of WT and solar PV subject to power-load balance and net-zero carbon criteria.

Figure 11 shows a 3-stage decision-making process which minimizes the non-

energy and energy cost sequentially in conjunction with the uncertain occurrences of DR requests. For Problems P2-1 and P2-2 which are linear integer programming models, they can be easily solved using off-the-shelf solvers or existing optimization tools. In Stage 3, given the optimal x_{jk} derived from P2-2, we search for optimal power capacity of WT and PV installation size to meet the energy requirements in each period of each week. The output power of WT and PV units is random and time-varying, so we propose a simulation based optimization algorithm to tackle Problem P2-3. The following three stage decision-making flow chart is presented:

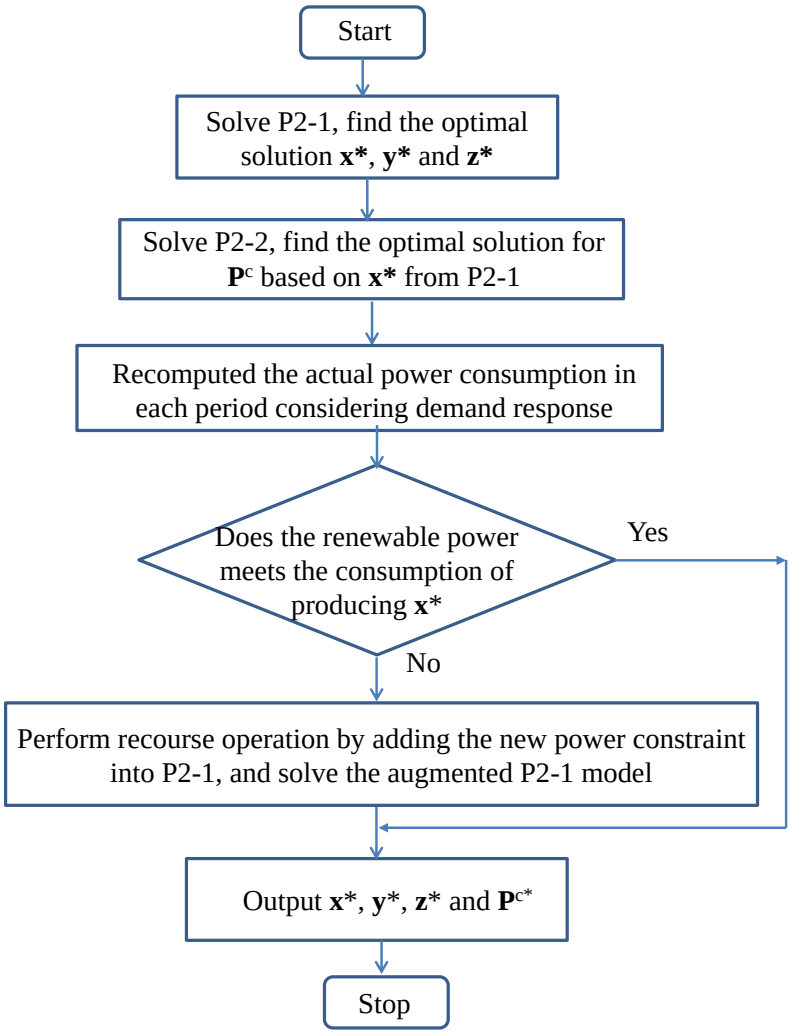

Figure 11. Flow Chart for Three-Stage Decision Model

If any of the stopping criteria is met, the presented algorithm is terminated and the result is reported as the final output. Otherwise, $\mathbf{x}_k$ and its simulated objective function value are added to the set of points available to build a new metamodel, and the main iteration will be repeated again. This proposed algorithm has been empirically shown to converge in a moderate number of iterations even in the presence of several variables using global optimization test functions (Villarreal et al. 2013).

The primary objective goal of Problem P1 is to determine the solar PV and WT capacities, namely $\mathbf{x}=\{x_1, x_2, \ldots, x_m\}$ and $\mathbf{P}^c=\{P_1^c, P_2^c, \ldots, P_m^c\}$, such that the system cost in Equation (12) is minimized. If x_i for i=3, 4,…, m are known, the capacity is also known. Hence, the actual number of decision variables is smaller than 2m. The simulation-based optimization is applied to determine the attractive DG solution for three different US fab sites in the following section.

Simulation-Based Optimization Algorithm

The algorithm firstly starts with an initial design of experiments from which an incumbent solution is obtained. At each iteration a metamodel is obtained using the available set of points and is used to generate a new attractive point where a simulation is performed. A metamodel can be defined as a model created with data generated through another model. An example of the former is a regression equation and an example of the latter is a computer model. For updating purposes, the simulated value of the new point is compared with the incumbent. A series of stopping criteria are evaluated and the new point is added to the existing data pool and a new

iteration should begin if none is met. Otherwise, the iteration stops.

Since Problem P1 contains random generated variables P_{it}, D_t and L_t, a search algorithm based on deterministic approach usually is not effective or cannot be directly used to solve the stochastic programming model. Simulation-based optimization is effective to find a good solution that is hopefully near the true, yet unknown, optimal solution. This algorithm has been empirically shown to converge in a moderate number of iterations (Floudas and Pardalos 1992, Karwan and Keblis 2007). Therefore, we adopt this optimization technique to seek the optimal solution for $\mathbf{P}^c$. Since there are only two decision variables, P_1^c for WT and P_2^c for PV, in the DG system, the optimization procedure can be implemented by combing the enumeration with the simulation.

Figure 12 depicts the flow chart of the optimization procedure. First, initial values are assigned to P_1^c, P_2^c, P_1^{max}, P_2^{max}, and ΔP. These values can be easily determined based on the mean load of the facility. Second, at time t renewable energy output from WT and PV is calculated according to simulated wind speed and weather patterns using equations (30) and (38). Based on equation (12), the DG power is compared with the hourly load to determine whether energy should be imported from or exported to the main grid. When t reaches 8,760 hours, objective function (12) and constraint (13) are assessed to determine whether current values of P_1^c and P_2^c meet the emission criterion or not. If criterion is met, the current P_1^c and P_2^c are treated as a candidate solution, and the LCOE is computed as well. By increasing P_1^c and P_2^c sequentially, a series of generation scenarios are obtained along with different LCOE.

Finally, the capacity mix of WT and PV that results in the minimum LCOE and zero-carbon emissions is chosen as the optimal solution. In order to obtain a robust design, for a given pair of P_1^c and P_2, the simulation is repeated for 20 years and the average cost is taken as the expected LCOE.

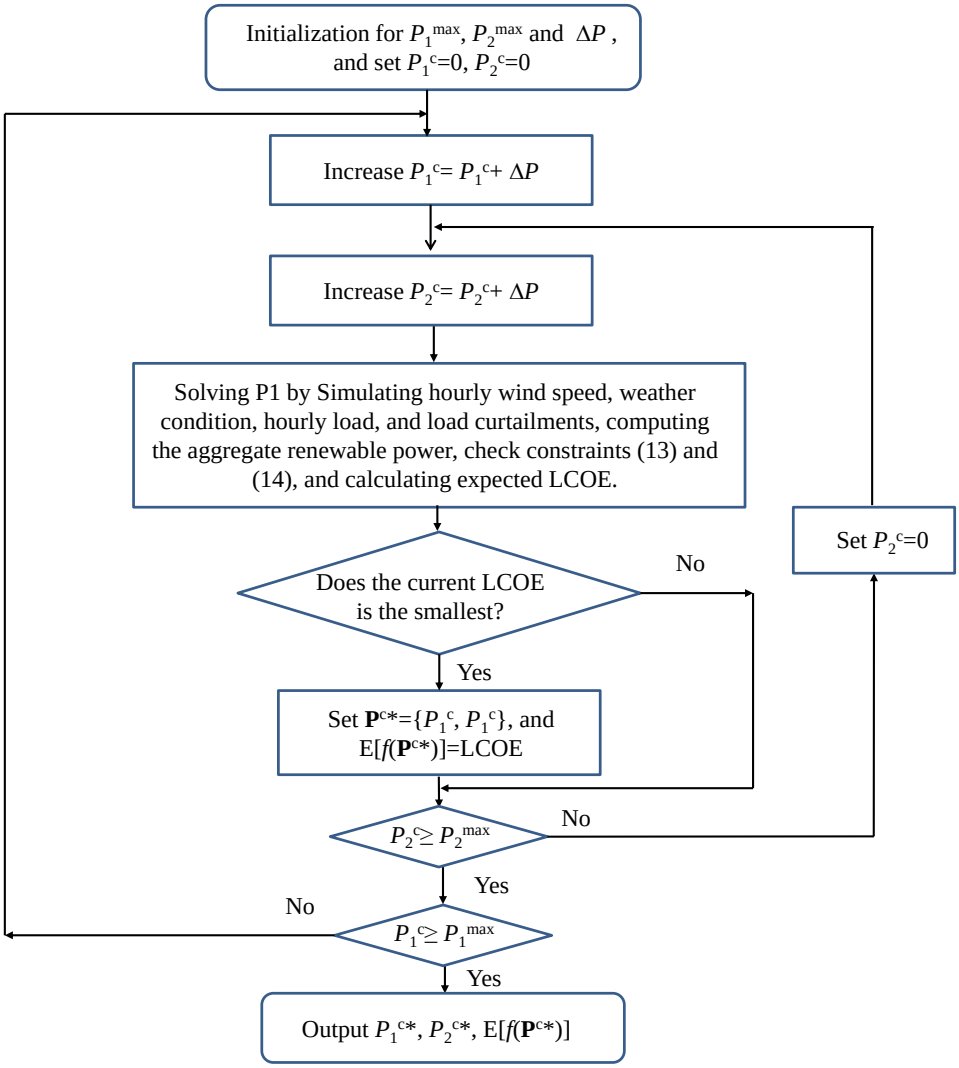

Figure 12. Simulation-based Optimization Algorithm

Wind Power Generation Model

Let v be the realization of the wind speed at time t, and $P_w(v)$ be the WT output power at v. Then $P_w(v)$ can be modeled by following cubic function (Jangamshetti and Rau 2001)

$$P_w(y) = \begin{cases} 0 & 0 < v < v_c, \text{ or } v > v_s \\ P_m\left(\dfrac{v}{v_r}\right)^3 & v_c \le v \le v_r \\ P_m & v_r \le v \le v_s \end{cases} \quad (30)$$

where, P_m is the rated power or the WT capacity. Note that v_c is the cut-in speed, v_r is the rated speed, and v_s is the cut-off speed. Figure 13 shows WT operates in one of the following states: 1) stationary without power generation when $v<v_c$; 2) non-linear power generation when $v_c \le v \le v_r$; 3) constant power output when $v_r \le v \le v_s$; and 4) shutdown if $v>v_s$ in order to protect motors. It has been shown that wind speed in a particular area can be fit with either Weibull or normal distributions (Weekes and Tomlin 2014, Karki et al 2006). The two-parameter cumulative Weibull distribution function for wind power generation is given as

$$F_w(v) = 1 - \exp\left(-\left(\frac{v}{c_w}\right)^{d_w}\right), \quad (31)$$

where c_w and d_w are the scale and the shape parameters, respectively. Equation (30) allows us to simulate the hourly wind speed based on the value of c_w and d_w that can be estimated from historical wind data.

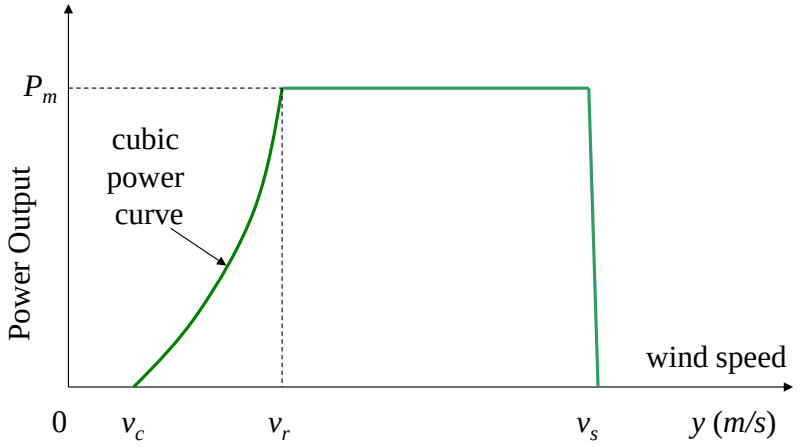

Figure 13. Wind Power Generation

Solar PV Generation Model

In theory, the output power of a PV system can be precisely predicted under the clear sky condition. The power intermittency has to do with the random behavior of the weather (e.g. partial cloud, cloud). Factors that have the main influences on the PV generation is summarized in Table 2. Note that the unit of the angles is radians unless specially indicated.

Table 2. Key Parameters in Solar PV Energy Production

No.	Factor	Symbol	Explanation
1	calendar day	d	$d \in \{1, 2, \ldots, 365\}$
2	local hours	t	t=1, 2, …, 24
3	solar hour (rad)	ω_t	related to the local hour
4	weather condition in hour h	W_t	random variable between [0, 1]
5	PV size (m^2)	A_s	PV module area
6	PV efficiency	η_s	between 10-20%
7	PV temperature (^{o}C)	T_o	operating temperature
8	latitude (rad)	ϕ	depends on location
9	PV azimuth angle (rad)	α	if facing south, α=0
10	PV tilt angle (rad)	β	between PV and ground

According to Figure 14, we present a three-step procedure to calculate the hourly PV energy production based on the early studies in Cai et al. (2010) and Taboada et al. (2012). These steps are summarized as follows:

Step 1: Compute the sunrise and sunset time for day $d \in \{1, 2, \ldots, 365\}$

$$\cos(-\omega_{rise}) = \cos(\omega_{set}) = \tan(\varphi - \beta)\tan\delta, \tag{32}$$

With $$\delta = 0.40928 \sin\left(\frac{2\pi(d+284)}{365}\right) \quad (33)$$

where δ is the solar declination angle, ω_{rise} and ω_{set} are the sunrise and the sunset angles in day d perceived from the PV panel. There is no power output for PV when $\omega < \omega_{rise}$ or $\omega > \omega_{set}$, i.e. before sunrise and after subset.

Step 2: Computing the total amount of solar irradiance incident on the PV surface at a particular time of a day

$$I_t = 1370\left(0.7^{(\cos\varphi)^{-0.678}}\right)\left(1+0.034\cos\left(\frac{2\pi(d-4)}{365}\right)\right)\times\left(\cos\theta + 0.1\left(1-\frac{\beta}{\pi}\right)\right) \quad (34)$$

With

$$\cos\varphi = \cos\delta\cos\phi\cos\omega(h) + \sin\delta\sin\phi, \quad (35)$$

$$\begin{aligned}\cos\theta = {} & \sin\delta\sin\phi\cos\beta - \sin\delta\cos\phi\sin\beta\cos\alpha + \cos\delta\cos\phi\cos\beta\cos\omega_t \\ & + \cos\delta\sin\phi\sin\beta\cos\alpha\cos\omega_t + \cos\delta\sin\alpha\sin\omega_t\sin\beta\end{aligned} \quad (36)$$

where I_t is the solar irradiance (W/m^2) received by the PV at time t on day d. Here φ is the solar zenith angle which is given by equation (34), and ω_t is the solar hour angle determined by the local clock time t. For instance ω_t=-π/2 at 6am in the morning, and it increases 15 degrees every hour until reaching ω_t=π/2 at 6pm in the evening. To maximize the energy throughput, PV panels located in the north hemisphere shall be oriented towards the south (i.e. α=0), then equation (35) can be simplified as

$$\cos\theta = \sin\delta\sin(\phi-\beta) + \cos\delta\cos(\phi-\beta)\cos\omega_t \quad (37)$$

Step 3: Under weather uncertainty, the actual power output of a PV system at time t, denoted as P_t in watts (W), now can be estimated as

$$P_t = W_t\eta_s A_s I_t\left(1-0.005(T_o-25)\right), \quad (38)$$

where W_t is a random variable representing the stochastic weather condition at time t

of day d, and varies between 0 and 1 to mimic an overcasting, partially cloudy, or clear day (Lave and Kleissl 2011). Note that A as the panel size (in m^2), T_o as the PV operating temperature (^oC) at time t, and η as the PV efficiency.

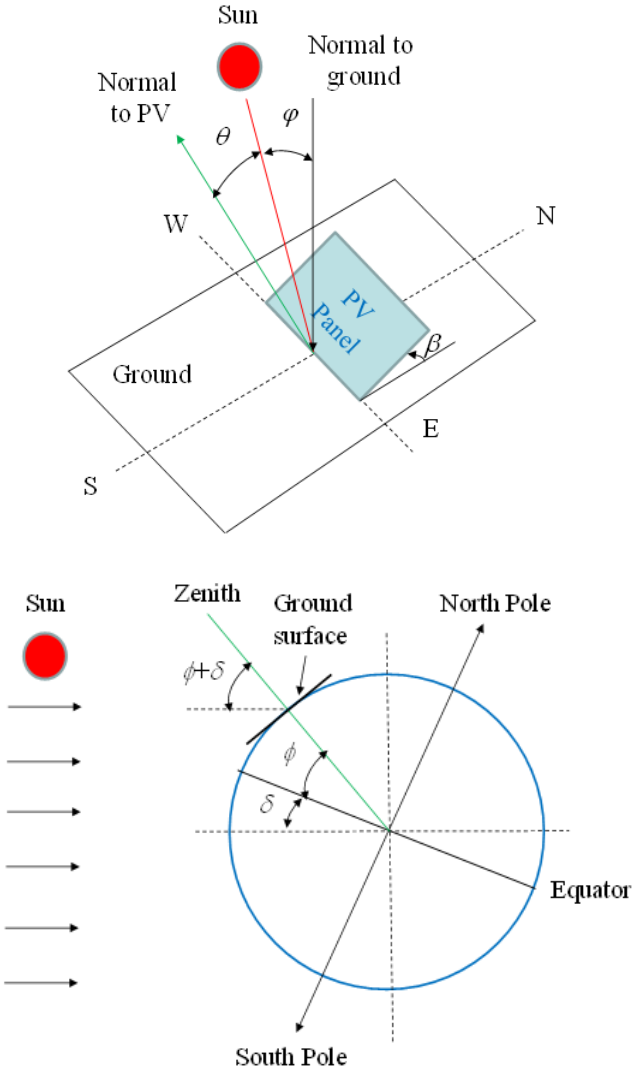

Figure 14. Working Principle of Solar PV during the Day

CHAPTER IV

SUPPORT VECTOR REGRESSION ENABLED ALGORITHM

Model-free algorithms such as GA, ANN and DOE often randomly search for optimal parameters based on experimental results. Such low efficient algorithms can only be implemented off-line. To increase the parameter optimization efficiency, a model based method is proposed to solve the modeling and parameter optimization problems based on the observed system input and output, and improve the manufacturing performance online.

SVR was first introduced by Vapnik, Steven Golowich, and Alex Smola in 1997 (Vapnik et al. 1997). The rapid development of SVR in statistical learning theory has motivated the researchers applying SVR to various fields. For now, it is widely used for wind speed prediction (SalcedoSanz et al. 2011), motherboard shipments forecasting (Wang et al. 2014), flood stage forecasting (Yu et al. 2006), and others. Therefore, we choose SVR to investigate the relationship between the assembly performance and its process parameters.

Support Vector Regression for Assembly Parameter Optimization

Given a set of assembly data $\{(x_1, y_1), (x_2, y_2), ..., (x_n, y_n)\}$, each $x_i \in R^n$ is the input vector and has the corresponding cycle time $y_i \in R$ for i = 1, 2,...,l, where n corresponds to the size of the training data set. The main objective of $\varepsilon - SV$ regression is to find a function $f(\mathbf{x})$ that has the deviation ε from the output cycle time for y_i the assembly data, and is as flat as possible at the same time. To achieve this objective, SVR maps the input data into a high dimensional feature space via a

nonlinear mapping and performs a linear regression in this feature space, i.e.,

$$f(\mathbf{x}) = \mathbf{w}^T ?\Phi(\mathbf{x}) + b \tag{39}$$

Where $\Phi(\mathbf{x})$ is called the feature; b is the bias term and $\boldsymbol{w}$ is the weight vector in the primal weight space. Flatness in (1) means that $\boldsymbol{w}$ should be as small as possible. We use Vapnik's ε-insensitive loss function (Drucker, 1997) defined as:

$$\left| f(\mathbf{x}_i) - y_i \right|_\varepsilon = \begin{cases} \left| f(\mathbf{x}_i) - y_i \right| - \varepsilon, \text{for} \left| f(\mathbf{x}_i) - y_i \right| \geq \varepsilon \\ 0, \qquad\qquad \text{otherwise} \end{cases} \tag{40}$$

Which means there exists a loss function that is capable of approximating all pairs $(\mathbf{x}_i, y_i)$ with ε precision. Our goal is to find the value of $\boldsymbol{w}$ and b such that the following regularized risk functional is minimized:

$$R_{ref}(f) = \frac{1}{2}\mathbf{w}^T\mathbf{w} + C\sum_{i=1}^{l} \left| f(\mathbf{x}_i) - y_i \right| \tag{41}$$

Where constant C>0 determines the tradeoff between the flatness of f and the amount of deviations larger than ε are tolerated.

The following minimization problem is formulated by introducing the slack variables ξ_i and ξ_i^*:

$$\begin{aligned} \underset{\mathrm{w},\xi_i,\xi_i^*}{\text{minimize}} \quad & \frac{1}{2}\mathbf{w}^T\mathbf{w} + C\sum_{i=1}^{l}(\xi_i + \xi_i^*) \\ \text{subject to} \quad & y_i - (\mathbf{w}^T ?\Phi\ \mathbf{x}_i\ + b\ \leq \varepsilon + \xi_i \\ & (\mathbf{w}^T ?\Phi\ \mathbf{x}_i\ + b\ - y_i \leq \varepsilon + \xi_i^* \\ & \xi_i, \xi_i^* \geq 0, i = 1, 2, ..., l \end{aligned} \tag{42}$$

A standard dualization method utilizing Lagrange multipliers is used to extend SVR. A Lagrange function is constructed by combining the objective function with the associated constraints. It can be shown that this function has a saddle point with respect to the primal and dual variables at the solution (Smola et al. 2004).

$$L := \frac{1}{2}\mathbf{w}^T\mathbf{w} + C\sum_{i=1}^{l}(\xi_i + \xi_i^*) - \sum_{i=1}^{l}\alpha_i(\varepsilon + \xi_i - y_i + \mathbf{w}^T\Phi(\mathbf{x}_i) + b) - \sum_{i=1}^{l}\alpha_i^*(\varepsilon + \xi_i^* + y_i - \mathbf{w}^T\Phi(\mathbf{x}_i) - b) - \sum_{i=1}^{l}(\eta_i\xi_i + \eta_i^*\xi_i^*) \quad (43)$$

Here L is the Langrangian and $\eta_i, \eta_i^*, \alpha_i, \alpha_i^*$ are dual variables satisfying positivity constraints, i.e. $\alpha_i^{(*)}, \eta_i^{(*)} \geq 0$. We refer to α_i^* and α_i by $\alpha_i^{(*)}$.The partial derivatives of L should satisfy the following conditions where the dual variables vanish at the optimality:

$$\frac{\partial L}{\partial b} = \sum_{i=1}^{l}(\alpha_i^* - \alpha_i) = 0 \quad (44)$$

$$\frac{\partial L}{\partial \mathbf{w}} = \mathbf{w} - \sum_{i=1}^{l}(\alpha_i - \alpha_i^*)\Phi(\mathbf{x}_i) = \mathbf{0} \quad (45)$$

$$\frac{\partial L}{\partial \xi_i^{(*)}} = C - \alpha_i^{(*)} - \eta_i^{(*)} = 0 \quad (46)$$

By eliminating the dual variables, the dual form of the nonlinear SVR can be expressed as:

$$\underset{\alpha_i, \alpha_i^*}{\text{minimize}} \sum_{i,j=1}^{l}\frac{1}{2}(\alpha_i - \alpha_i^*)(\alpha_j - \alpha_j^*)\left(\Phi(\mathbf{x}_i)\Phi(\mathbf{x}_j)\right) + \varepsilon\sum_{i=1}^{l}(\alpha_i + \alpha_i^*) - \sum_{i=1}^{l}y_i(\alpha_i - \alpha_i^*) \quad (47)$$

$$\text{subject to } \sum_{i=1}^{l}(\alpha_i - \alpha_i^*) = 0 \text{ and } \alpha_i, \alpha_i^* \subset [0, C]$$

The minimization function has the following form:

$$\mathbf{w} = \sum_{i=1}^{l}(\alpha_i - \alpha_i^*)\Phi(\mathbf{x}_i) \quad (48)$$

$$f(\mathbf{x}, \alpha_i, \alpha_i^*) = \sum_{i=1}^{l}(\alpha_i - \alpha_i^*)k(\mathbf{x}_i, \mathbf{x}) + b \quad (49)$$

Where the kernel function $k(\mathbf{x}_i, \mathbf{x})$ is the inner product of the nonlinear mapping

$$k(\mathbf{x}_i, \mathbf{x}) = \Phi(\mathbf{x}_i)?\Phi\ \mathbf{x} \tag{50}$$

In a sense, the number of Supports Vectors with no vanishing coefficients conduces to the complexity of the function's representation.

Variable *b* can be computed based on Karush-Kuhn-Tucker (KKT) condition (Lasserre et al. 2001), which implies that the product of the Lagrange multipliers and constrains has to be equal to zero.

$$\begin{aligned} \alpha_i(\varepsilon + \xi_i - y_i + \mathbf{w}^T?\Phi\ \mathbf{x}_i\ + b\ = \\ \alpha_i^*(\varepsilon + \xi_i^* + y_i - \mathbf{w}^T?\Phi\ \mathbf{x}_i\ - b\ = \end{aligned} \tag{51}$$

Where $(C-\alpha_i)\xi_i = 0$ and $(C-\alpha_i^*)\xi_i^* = 0$. For all samples inside the tube ε, $\xi_i = \xi_i^* = 0$. Then the variable *b* can be calculated as following:

$$\begin{aligned} b &= \varepsilon + y_i - \mathbf{w}^T\ \Phi(\mathbf{x}_i) \quad \textit{for } \alpha_i \in (0, C) \\ b &= -\varepsilon + y_i - \mathbf{w}^T\ \Phi(\mathbf{x}_i) \quad \textit{for } \alpha_i^* \in (0, C) \end{aligned} \tag{52}$$

The number of Supports Vectors (SVs) with nonvanishing coefficients conduces to the complexity of a function's representation by SVs.

Hyperparameters optimization

Some common kernels are shown in Table 3. Among the four kernels, Gaussian Radial Basis Function kernel (RBF) can nonlinearly map the samples into a high dimension of space and has fewer hyper parameters which reduce the influence on the complexity of model selection than the Polynomial kernel. Therefore, we choose RBF in this research, which is commonly used as the kernel for regression.

Table 3. Covariance Functions

Name	Equation
Linear	$k(\mathbf{x}_i, \mathbf{x}_j) = \mathbf{x}_i \cdot \mathbf{x}_j$
Polynomial	$(k(\mathbf{x}_i, \mathbf{x}_j) = \left[\gamma(\mathbf{x}_i \cdot \mathbf{x}_j + c \right]^d$
Sigmoid	$(k(\mathbf{x}_i, \mathbf{x}_j) = \tanh\left[\gamma(\mathbf{x}_i \cdot \mathbf{x}_j + c \right]$
Radial Basis Function	$k(\mathbf{x}_i, \mathbf{x}_j) = \exp(-\gamma \left\| \mathbf{x}_i - \mathbf{x}_j \right\|^2)$

The nonlinear SVR with Gaussian RBF kernel includes three hyper parameters: the constant value *C*, the radius of the insensitive tube ε and the kernel parameter γ. These are independent parameters and the different combinations of the parameters will lead to different SVR models with different specialty. A large *C* value means a greater penalty of errors, which makes the learning machine process more complex. However, a smaller *C* tolerates excessive errors with poor estimation. If *C* goes to infinity, SVR would not tolerate any error and result in a complex model; if *C* goes to zero, a large amount of errors are allowed and the model would be less complex (Xuegong et al. 2000). The parameter ε is also an important hyper parameter since it governs the accuracy and complexity of the approximation function because a smaller ε results in a complex supervised learning machine process.

Several methods have been proposed to optimize this process. Manual search and particle swarm optimization are introduced based on user's prior knowledge and/or expertise, which are obviously not appropriate for non-expert users and have the chance to find the local optimum. Grid search is reliable in low dimensional spaces and suffers from the curse of dimensionality. Random search, which is independently

drawn from a uniform density, has all the practical advantages of grid search while it obtains a large improvement in efficiency in high-dimensional search spaces.

In this work, we use grid search to locate the range of the optimal parameter variations without any prior knowledge. Then random search integrated with cross validation is utilized to find the best combination of hyper parameters for the SVR model (RS-SVR). For comparison, a finer grid search after using a coarse grid is conducted on the neighborhood to find the best hyper parameters with the highest cross validation rate to model the complex assembly process (GS-SVR). To reduce the calculation complexity of the learning machine, we first set a real value for the constant value *C* and then use grid search together with random search to select the best combination for ε and λ.

The constant value *C* can be chosen to be equal to the range of output values of training data (Mattera et al. 1999). However, such a selection of *C* is quite sensitive to possible outliers (in the training data), so the following prescription is proposed:

$$C = \max(|\bar{y} - 3\sigma_y|, |\bar{y} + 3\sigma_y|) \tag{53}$$

where $\bar{y}$ is the mean of the output of training data; σ_y is the corresponding standard deviation.

SVR Enabled Algorithm

An online robotic assembly process is a high-dimensional, continuous, nonlinear process which must be monitored and controlled in a real-time manner. To that end, the system is expect to make quick response to any performance variations. To solve this type of complex problems, it is imperative to make a dynamical trade-off between

exploration and exploitation (Lifeng et al. 2011). We jointly use exploration and exploitation processes to carry out system modeling and parameter optimization. The drawback is that the optimization process can be easily trapped in local minimum if both processes are not properly adjusted. Hence in the proposed algorithm, exploration and exploitation should be balanced to facilitate the simultaneous online modeling and optimization. Meanwhile, a switching criterion is also necessary to alleviate the computational complexity of SVR.

Exploration and Exploitation

In this research, we utilize SVR enabled algorithm to iteratively model a complex system and optimize the system performance. In each iteration, new samples are added into the existing data pool and the SVR model is also updated based on the aggregate data. Then the new SVR model will be used to search for the global optimum by minimizing a function for which a specific location is chose for sampling. This function is called acquisition function. The purpose of acquisition function is to guide the search for the optimum controls of the new sample points. It directly affects the model quality and the optimal solution. Therefore, it plays a pivotal role in the SVR enabled algorithm during the optimization process because the combination of the acquisition function and SVR allows for a trade-off between exploration and exploitation to search for the optima.

If the optimal parameters found by SVR are returned with a longer assembly cycle time than what is required, the proposed algorithm can automatically re-search for the entire sampling space to enrich the information for the SVR model until the

global optimal parameters are found. To deal with such problems, we propose to use λ-Greedy acquisition function:

$$AC(\mathbf{x}) = \begin{cases} \hat{y}(\mathbf{x}) & \text{rand}(1) > \lambda \\ \arg\max \min_{i \in 1...N} [d(\mathbf{x} - \mathbf{x}_i)] & otherwise \end{cases} \quad (54)$$

According to the acquisition function, the new candidate is generated by using $\mathbf{x}^* = \arg\min AC(\mathbf{x})$, where λ is the performance index updated online according to the hyper parameters and system performance; $d(\mathbf{x} - \mathbf{x}_i)$ is the distance between two sets of parameters $\mathbf{x}$ and $\mathbf{x}_i$; $\hat{y}_x$ is the predicted cycle time with a certain assembly parameters $\mathbf{x}$. During the iteration, if $\text{rand}(1) > \lambda$, the new candidate is optimized by utilizing the current model for exploitation process of the process parameters; otherwise, the exploration process is activated to refine the model by exploring the sample space.

Adaptive Optimization Process

The performance of the robotic assembly is often measured by the assembly cycle time and FTT rate. The FTT rate and the average cycle time can be computed upon the completion of several assembly tasks. If both measurements satisfy the pre-specified criteria, the production process begins; otherwise, the assembly process model continues to be updated until the required criteria are satisfied. To reduce the computational complexity, the optimization process should be terminated once the model becomes stable and the optimal parameters are found. The production activities are executed repeatedly with the obtained optimal assembly process parameters. If the system performance decreases, the optimization process should be triggered to re-optimize the process parameters until it meets the stopping criteria.

To lower the assembly failure rate, prior information about the cycle time variance is required. However, for different batches or assembly processes, such information usually is different to obtain. Technically assembly failures are inevitable because of environmental changes during assembly processes, which makes the recorded cycle time for modeling unreal. Nevertheless, existing methods like DOE eliminate these data set even though that information is useful for modeling and optimization of assembly process. Hence we proposed a switching criteria to control the parameter optimization process:

$$\lambda = \begin{cases} 1 & \alpha > 1 \\ 0 & \alpha < k_3 \text{ and } C_t < C_t^* / k_1 \text{ or FTT} > \beta_t \\ 0.5 & \alpha < k_3 \text{ and } C_t > C_t^* / k_2 \text{ and FTT} < \beta_t \\ \alpha & \text{otherwise} \end{cases} \tag{55}$$

where λ is the switching parameter; k_1 and k_2 are two constants controlling the optimization process; k_3 is the threshold that determines whether a model has already converged; C_t^* is the best cycle time so far and C_t is the current cycle time; β_t is the acceptable FTT rate defined by the user which is calculated until the system is in production process. Otherwise, β_t is set to 1 during the optimization process. $\alpha = |H_k - H_{k-1}| / |H_k - H_0|$ is the normalized change of hyper parameters, where H_k is the hyper parameters at iteration *k*. If a model converges, $\alpha \to 0$. If $\alpha > 1$, the switching parameter λ is set to 1 to explore the optimal solution in the sample space; When λ and cycle time satisfy the given criteria required by assembly process, λ is set to 0 to begin productive process using optimized assembly process parameters. T he production process is continuously monitored by α, cycle time and FTT rate. If the performance degrades, α is set to 0.5 to restart the optimization process;

otherwise λ is set to α for balancing the exploration and exploitation processes.

CHAPTER V

ZERO-CARBON EMISSION ANALYSIS

Background information

We investigate whether a net-zero carbon production system can be realized through onsite wind-solar generation in different regions of the world. In particular, ten cities from different regions around the world are selected to represent the diversity of wind profiles and weather patterns. Data associated with the latitude, the mean and the standard deviation of wind speed, and the percentage of sunny, partially cloudy and overcast days are summarized in Table 4 which is repossessed through National Climate Date Center (NCDC 2014) and Weather Underground (WU 2014), correspondingly. Only one city is located in the southern hemisphere, and the rest are from the northern hemisphere. The latitude of these cities varies from 18.25 to 51.63 degrees, covering the majority areas of the human beings residence. Cities like Wellington possesses large wind profile but with less sunny days. Cities like Sanya and Phoenix have the largest number of sunny days but with moderate or small wind power. Other cities such as Shanghai and Munich receive moderate sunshine as well as medium wind power. These wind and climate data allows us to simulate hourly wind speed y and the daily weather factor W_t, which is further used to predict the WT and PV output based on Equations (29) and (37). We search for the optimal x_{jk}, y_{jk}, z_{jk}, P_1^c, and P_2^c in each location such that the 100% GEC goal is achieved while the annual production-inventory cost is minimized.

Table 4. Wind Speed Profile and Weather Pattern of Testing Cities

No	City	Country	Latitude (degree)	AWS (m/s)	SWS (m/s)	Sunny (days)	PC (days)	Overcast (days)
1	Rio Gallegos	Argentina	51.63	7.16	1.07	144	84	137
2	Shanghai	China	31.20	4.43	1.85	181	41	140
3	Sanya	China	18.25	6.51	3.11	235	42	88
4	Munich	Germany	48.13	5.14	1.04	65	110	190
5	Tokyo	Japan	35.68	5.22	0.40	179	22	164
6	Wellington	New Zealand	41.29	8.05	1.21	79	100	186
7	Phoenix	USA	33.30	2.78	0.32	211	85	70
8	Boston	USA	42.36	5.68	0.56	168	64	133
9	Honolulu	USA	21.30	5.09	0.50	169	39	157
10	New York	USA	40.71	5.30	0.60	107	102	156

Note: AWS=average wind speed, SWS=standard deviation of wind speed, PC=partially cloudy

The proposed DG system is comprised of WT generators and solar PV panels. The WT's cut-in, rated and cut-off wind speeds are v_c=2, v_r=10, and v_s=25 m/s, respectively. The efficiency of PV module is η=0.15, and the average operating temperature is T_o=45 ^{o}C. We assume that the pay-off period of WT and PV equipment is n=20 years, and the annual interest rate is r=0.05. For the DR program, it is assumed that contingency calls follow the distribution of Poisson process with λ=5 events/year. The maximum curtailment duration for one event is 8 hours, and the

curtailment level is 20 percentage of the mean load. Parameters and cost items related to WT and PV units are listed in Table 5, and these values are derived based on extant literature (Fingersh et al. 2006, Timilsina et al. 2012). These values are estimated based on existing literature with the best effort to reflect the real-world situations as closely as possible (Fingersh et al. 2006, Freris and Infield 2008).

In this section, we carried out a comprehensive numerical experiment to test the zero-carbon production-inventory decision model proposed in Problem P2. Certain parameters such as carbon credits and production losses may vary with regions or business sectors. Hence the lower and upper limits are presented to capture the possible range of these parameters.

Table 5. Cost Parameters and Related Data for WT and PV

Notation	Meaning	Value
a_1	Capacity cost of WT ($/MW)	1.5×10^6
a_2	Capacity cost of PV ($/MW)	3.5×10^6
b_1	O&M cost of WT ($/MWh)	5
b_2	O&M cost of solar PV ($/MWh)	2
c_1	Carbon credits of WT ($/MWh)	0, 10
c_2	Carbon credits of solar PV ($/MWh)	0, 20
T	DG system loan payment period (years)	20
θ	Annual interest rate	0.05
ε	production loss in DR ($/MWh)	10^4, 10^5
ρ	price of grid electricity ($/MWh)	60
q	net metering rate ($/MWh)	60
λ	load curtailment occurrence rate (calls/year)	5
η_s	PV efficiency	0.15
T_o	PV operating temperature (^{o}C)	45
γ	loss-of-load-probability criterion	0.001
v_c, v_r, v_s	cut-in, rated and cut-off wind speeds (m/s)	2.5, 10, 25

We summarizes the necessary parameters pertaining to the multi-period, production-inventory planning model in Table 6. The virtual production facility belongs to industry sectors that are heavily dependent on electricity as their primary energy source (e.g. semiconductor production, plastics, vehicle manufacturing, and chemical processing). In this example, we assume the manufacturing facility is

capable of making two product types (Product 1 and Product 2), and the planning horizon is 52 weeks (or one year) with one week per period. Besides the energy and materials consumption, other resources involved include the labors and machines. The demand for products 1 and 2 of each period follows the normal distribution with (μ_1=1,000, σ_1=150) and (μ_2=600, σ_2=60), respectively.

Table 6. Non-Energy Cost and Parameters for Production-Inventory System

Notation	Meaning	Value
j	index for product type, we consider two product types	j=1, 2
k	index for production period, we consider 52 weeks	k=1, 2,…, 52
τ	number of hours in a production period (hours)	168
d_{jk}	demand for product j in period k	normally distributed
c_{jk}	material and labor cost of making product j in period k ($)	c_{1k}=500, c_{2k}=700
h_{jk}	unit holding cost for product j in period k ($/period)	h_{1k}=100, h_{2k}=140
b_{jk}	backorder cost for product j in period k ($/item)	b_{1k}=1000, b_{2k}=1400
r_{js}	non-energy resource s involved for making one unit of product j, where s=1 for labor and s=2 for machine	r_{11}=4, r_{21}=6, r_{12}=10, r_{22}=20,
w_{sk}	capacity limit for resource s in period k (hours)	w_{1k}=9000, w_{2k}=2500
e_j	amount of energy consumed for making one unit of product j (MWh/item)	e_1=0.9, e_2=1.2

Firstly, we compute the production-inventory system without carbon credits, and the production losses are equal to 100,000 $/MWh. Based on the data in Tables 2 and 3, we compute the installation capacity of WT and PV in each location, and the results are listed in the following tables. At the meantime, we also compute the levelized cost of energy (LCOE) at each location, LCOE is defined as follows

$$LCOE = \frac{C_{DG}(\mathrm{P}^c)}{\sum_{t=1}^{h}\sum_{i=1}^{g} P_{it}}, \tag{56}$$

where CDG(Pc) is given in Equation (8), and the dominator represents the annual renewable energy generated by the onsite DG system.

The monthly load profile of the virtual manufacturing facility follows the normal distribution with the mean and the standard deviation shown in Table 1. Based on Problem P1, we search the optimal WT and PV combination such that the facility achieves net-zero carbon emission performance with the minimum LCOE. The simulation-based optimization algorithm is used to solve the proposed scholastic programming model, and the detailed search method is implemented using Matlab. We further classify the DG planning into four cases based on different carbon credit policies and operating modes (see Table 7). For Case 1, it serves as the benchmark analysis with no carbon credits to wind and solar energy. In Cases 2 and 3, carbon credits are taken granted to WT and PV, respectively. In Case 4, we assume the facility only operates 12 hours a day from 7am to 7pm. We are intend to investigate whether solar PV is preferred over WT when a facility consumes the energy only in daytime.

Table 7. Carbon Credits and Operating Mode of Manufacturing Facility

Case	Operating Mode	Carbon credit of WT ($/MWh)	Carbon credit of PV ($/MWh)	Pricing Policy	Utility Rate ($/MWh)
1	24/7	0	0	fixed	70
2	24/7	35	0	fixed	70
3	24/7	0	35	fixed	70
4	24/7	0	0	TOU	35 and 70
5	24/7	0	0	POU	70 and 105
6	12/7	0	0	fixed	70

Results Analysis

In Case 1, we search for the optimal installation capacity of WT and PV that minimizes the LCOE in each city, and the results are summarized in Table 8. Three interesting observations are made according to these data. First, all locations except Phoenix are in favor of WT installation. Cities such as Sanya, Wellington and Rio Gallegos are able to achieve a cost-effective DG installation capability with LCOE of $48/MWh, $52/MWh and $60/MWh without carbon credits. These values are 30%, 26% and 14% lower than the utility rate of $70/MWh. This is largely due to the higher average wind speed in these sites coupled with low equipment cost of WT. Phoenix is the only city dominated by PV installation due to the strong sun shine with extremely lower wind speed. The LCOE in Phoenix reaches as high as $198/MWh because of the high equipment cost of PV. Manufacturers can also achieve net-zero carbon emission in cities where average wind speed between 4~6 *m/s*, yet the LCOE rises up by 35-72% compared with the normal utility rate. Notice that the relative cost difference (RCD) in Cases 1 is defined as RCD=(LOCE-70)/70. We also compare the

LCOE with the projected utility price after 20 years. It is estimated as $126/MWh assuming 3% annual increase. The result shows that the LCOE in other cities is less than the projected rate except for Phoenix. Obviously onsite generation allows manufacturers to increase cost independence from the volatile electricity market.

In Case 2, we minimize the LCOE of the DG system assuming that a carbon credit of $35/MWh because of WT installation. Likewise, in Case 3, we optimize the onsite DG system assuming that a carbon credit of $35/MWh is granted to PV installation. Table 9 presents the optimum resolution to WT and PV capacity and the LCOE for each city. It is thought-provoking to found that the installation of WT and PV in corresponding city remains almost the same by comparing Cases 2 and 3 with Case 1, indicating that carbon credit has a limited influence on the DG configuration. Nevertheless, carbon credit reduces the LCOE in locations where the subsidized generation technology is adopted. This example also shows that carbon credits alone may fail to stimulate onsite renewable integration unless it is aligned with the local wind speed and weather condition.

Table 8. Optimal WT and PV Capacity for Ten Cities in Case 1

No.	City	WT (MW)	PV (MW)	LCOE ($/MWh)	RCD (%)	Cost difference after 20 years ($/MWh)
1	Rio Gallegos	24.0	2.0	60	-14	-66
2	Shanghai	70.1	1.4	120	72	-6
3	Sanya	19.7	1.5	52	-26	-74
4	Munich	62.3	1.4	115	64	-11
5	Tokyo	66.0	1.0	115	65	-11
6	Wellington	17.0	1.5	48	-31	-78
7	Phoenix	1.3	49.2	198	184	72
8	Boston	50.4	1.4	94	35	-32
9	Honolulu	69.8	1.2	118	69	-8
10	New York	61.7	1.3	112	61	-14

Table 9. Optimal WT and PV Capacity in Cases 2 and 3 with Carbon Credits

		Case 2				Case 3			
No.	City	WT (MW)	PV (MW)	LCOE ($/MWh)	RCD (%)	WT (MW)	PV (MW)	LCOE ($/MWh)	RCD (%)
1	Rio Gallegos	24.0	2.0	24	-66	24.0	1.8	66	-6
2	Shanghai	70.5	1.5	84	21	69.9	1.7	116	66
3	Sanya	19.5	1.9	19	-72	19.6	2.0	52	-26
4	Munich	61.9	1.6	84	19	62.3	1.7	108	54
5	Tokyo	65.9	1.0	84	21	66.0	1.0	107	53
6	Wellington	17.0	1.5	17	-75	17.0	1.5	46	-35
7	Phoenix	1.8	48.7	197	181	1.0	49.3	160	129
8	Boston	50.3	1.5	63	-11	50.3	1.0	93	33
9	Honolulu	70.1	1.0	86	22	69.9	1.1	128	83
10	New York	61.9	1.1	75	7	61.8	1.2	106	51

In Cases 4 and 5, we reduce the LCOE of each city under TOU and POU pricing schemes. The results are plotted in Figure 15 in conjunction with Case 1 for comparison. Under the TOU policy, the utility company charges the manufacturer on the electricity based on when the energy is consumed. The rate is $70/MWh from 7AM and 7PM, and reduced by 50% from 7PM to 7AM. Technically TOU can incentivize large industrial consumers to shave the load curve by shifting the demand to the off-peak hours. Interestingly, if the primary onsite generation is WT units, our numerical example shows that TOU does not bring significant cost saving to a manufacturer. However, Phoenix (City 7) dominated by PV installation does benefit from the TOU policy as the LCOE is reduced by $36/MWh compared to its cost in Case 1. This is because the facility in Phoenix used to pay a flat electricity rate across 24 hours, now can reduce the payment by 50% in the night when PV power is not available. For cities dominated by wind power, the majority of the electricity in the night is supplied from WT. Thus TOU has little influences on the LCOE of these locations.

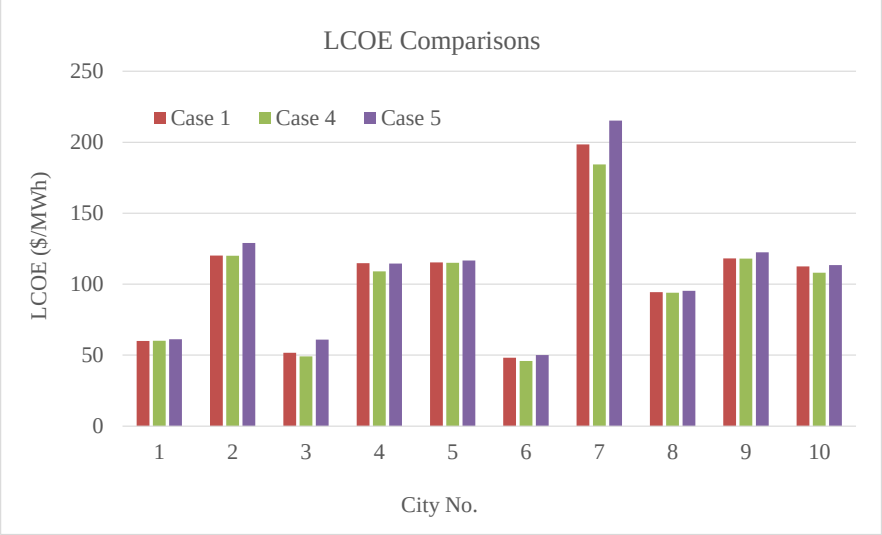

Figure 15. LCOE Comparisons (from left to right: Cases 1, 4, and 5)

In POU of Case 5, the utility's electricity price increases step-wise in accordance to the amount of the power drawn from the grid. A regular price which is \$70/MWh is imposed whenever the power load is below a certain level, say P_1. If the load to the grid is P_2 larger than P_1, a higher price is imposed on the extra portion that exceeds P_1. We set a quite stringent criterion in Case 5: as long as the load to the grid exceeds 20% of the mean load which is 9.587 MW, the rate is increased to \$105/MWh. It is quite surprising that cities dominated with WT installation, the incremental cost resulted from POU policy is almost negligible. However, the LCOE in Phoenix increases and reaches \$215/MWh, or \$17 higher than its baseline. This is because in Phoenix almost all the electricity to power the facility in the night must rely on the utility grid as there is no PV generation after the Sun sets down.

Table 10. Comparisons between Case 1 and Case 6 in Different Operating Modes

No.	City	Case 1			Case 6		
		WT (MW)	PV (MW)	LCOE (\$/MWh)	WT (MW)	PV (MW)	LCOE (\$/MWh)
1	Rio Gallegos	24.0	2.0	60	12.0	1.0	64
2	Shanghai	70.1	1.4	120	35.2	1.0	119
3	Sanya	19.7	1.5	52	9.7	1.4	51
4	Munich	62.3	1.4	115	31.1	1.1	116
5	Tokyo	66.0	1.0	115	33.0	1.0	113
6	Wellington	17.0	1.5	48	8.0	1.2	74
7	Phoenix	1.3	49.2	198	1.5	24.8	199
8	Boston	50.4	1.4	94	25.0	1.0	99
9	Honolulu	69.8	1.2	118	35.0	1.0	125
10	New York	61.7	1.3	112	30.6	1.3	112

In Case 6, we optimize the capacity of WT and PV assuming the manufacturing facility operates only 12 hours a day from 7AM to 7PM. Since the mean energy consumption is reduced by 50 percent compared to the 24/7 mode, the

capacity of WT and PV units in each location is only a half of the corresponding installation in Case 1 (see Table 8). This result seems contradictory because the facility consumes the electricity in the daytime, and more PV installation would be anticipated due to the availability of sun shine. This is true if the DG system is designed and operates in an islanding mode with no connection to the grid. However in a grid-connected DG system, it is the levelized cost of energy, not necessary the sun availability, eventually determines the generating type and capacity. This is because the DG system can import the electricity from the grid during the daytime, and return the energy to the grid in the night when the load is small. Whether a manufacturer decides to install WT or PV as the onsite generator is not dependent on the facility's operating model. Rather it is more related to the local wind speed and sunny days.

PV Capacity Cost vs. Penetration Rate

We are also interested in how the cost of PV equipment influences its penetration in the onsite energy portfolio. To answer this question, we sequentially reduce the PV capacity cost from $\$4\times10^6$/MW to $\$0.5\times10^6$/MW, and solve the DG planning model to obtain a set of optimal renewables capacity mix. It is anticipated that the PV penetration rate will increase with its reduced capacity cost. The penetration rate is defined as the PV capacity over the total DG capacity which is the sum of WT and PV units. We choose Shanghai and Munich as the candidate locations to analyze the PV penetration rate because both cities have moderate wind speed and weather condition. Figure 16 depicts the PV penetration rate versus its capacity cost for both cities. The PV penetration rate in Phoenix is also included for the purpose of

comparison. If the cost of PV is reduced to $\$2\times10^6$/MW, it can compete with wind energy in locations like Shanghai where the number of overcast days is 38 percent in a year. For locations where the overcast days exceed 50 percent in a year, the cost of the PV must be reduced to $\$1\times10^6$/MW in order to penetrate into the DG portfolio. If the PV cost can drop to $\$0.5\times10^6$/MW, it will displace the wind energy market in Shanghai, Munich, and other cities.

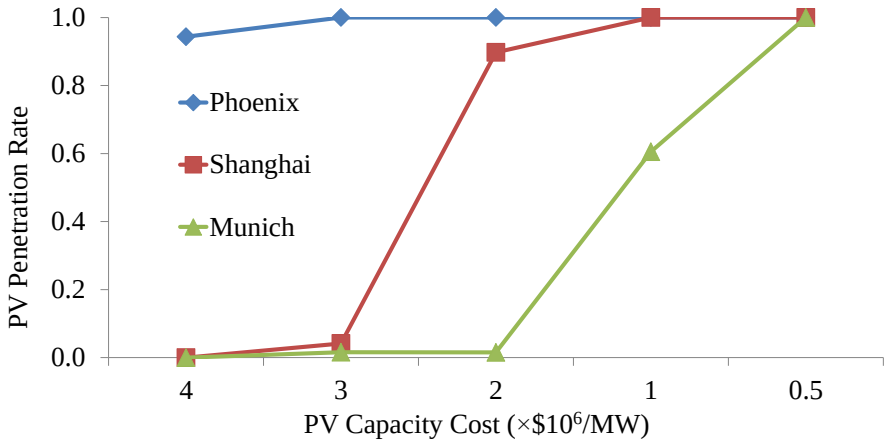

Figure 16. PV Penetration Rate vs. Capacity Cost

CHAPTER VI

INDUSTRIAL ROBOTIC ASSEMBLY EXPERIMENTAL RESULT

Industrial High Precision Robotic Assembly

Experiments on a high precision valve body assembly process, a typically peg-in-hole assembly process, are carried out to demonstrate the proposed method. The clearance between the peg and the hole is only $40\mu m$ which exceeds the motion accuracy of the industrial robot. The experimental system as shown in Figure 17 is consisted of an ABB IRB140 robot with a single cabinet IRC5 controller, an ATI Gamma force sensor fitted with the robot end effector. The value body is fixed on the steel table.

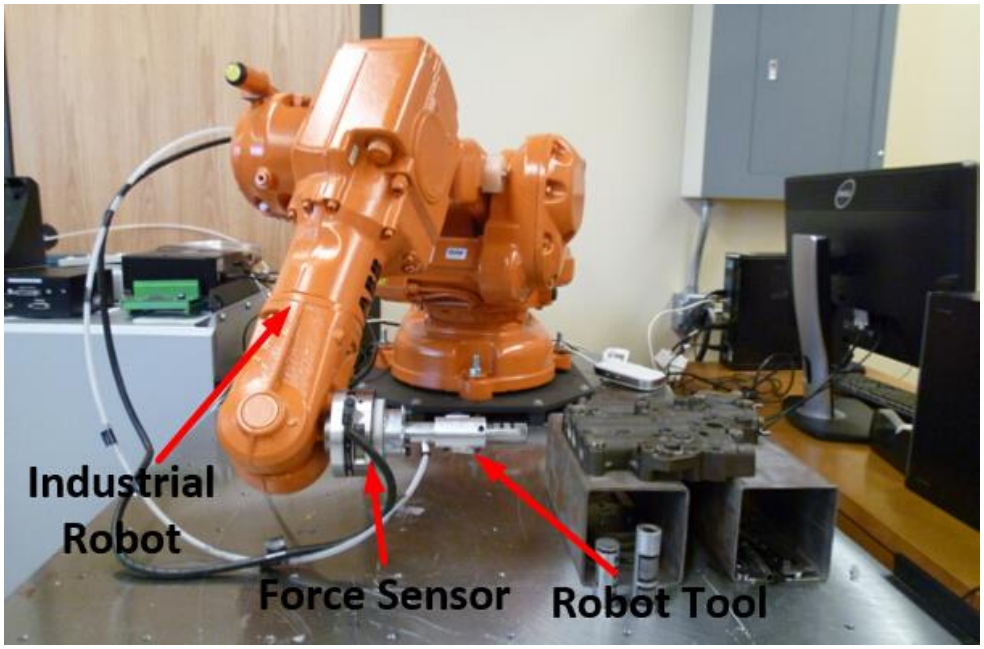

Figure 17. Experimental System

An external computer is connected to the robot controller via Ethernet link for real-time data communication. The two-way connection is able to send assembly parameters from the host PC to the controller, and to return real-time feedback data

from the controller to the PC. The ABB force control package is used to perform the assembly process. A robot program (ABB robot programming language, RAPID) has been developed to carry out the assembly process parameterization. Another RAPID program downloaded in the controller is to communicate with the external computer and generate robot force control parameters. A SVR enabled algorithm interacts with the force control assembly production program to switch the value of assembly related parameters from optimization to production and collect the experimental data. Experiments with different offsets are performed according to the assembly parameters for small and large work piece locations, respectively. The robot tool starts from a random position, contacts with the surface of the work piece and moves along a pattern. Once the tool approaches the vicinity of the hole, the tool can move forward. The movement is monitored by the force sensor and the search process terminates if the searching attempt fails.

The assembly process consists of force guided spiral search and force controlled linear move. There are four process parameters involved in the assembly process: search force (SF), search speed (SS), insertion force (IF) and search radius (SR). As listed in TABLE 1, four sets of experiments are performed for comparison purpose. SVR #1 refers to three parameters and each parameter has three values; SVR #2 refers to three parameters and each parameter has more than three values; SVR #3 refers to three parameters of different range and each parameter has more than three values. In Table 11, the parameters are defined using the format (Minimum Value: Interval: Maximum Value). The noise of the system is shown in Table 12, which is a random

uniform number between the minimum and maximum values.

Table 11. Parameter Configurations

Method	SS(mm/s)	SF(N)	IF(N)	SR(mm)
SVR #1	[250:50:350]	[5:15:35]	[50:25:100]	2
SVR #2	[250:10:350]	[5:0.5:35]	[50:5:100]	2
SVR #3	[200:10:300]	[10:0.5:40]	[25:5:75]	2
DOE	[250:50:350]	[5:15:35]	[50:25:100]	2

Table 12. System Noise of Online Assembly Process

Δx (mm)	Δy (mm)	q1	q2	q3
±1.5	±1.5	±0.001	±0.003	±0.001

The parameters in the algorithm are chosen as $k_1 = 0.9$, $k_2 = 0.7$, $k_3 = 0.05$, $\beta_t = 0.99$. From Equation (54), we know that the model will be converged when k_1 and k_3 are close to 1 and 0, respectively. Either α and current cycle time or FTT rate, which satisfies the given criteria, will keep the system in production process. The process parameter optimization should be restarted if the shortest cycle time recorded is less than 70% of the current cycle time and FTT rate under 99%. As for the hyperparameter of SVR, we choose ε between 0 and 5, and $\gamma \in [2^{-5}, 2^{5}]$.

In the DOE method, multiple values are chosen to test the parameter combinations in order to overcome the variations. The combination resulting in the minimum cycle time and variation is treated as the optimal parameters. Quite often a cross-functional team by quality engineers, software programmers and machine operators is needed to perform this kind of DOE optimization task. Compared with DOE methods, SVR enabled algorithm is capable of finding a set of optimal assembly parameters automatically in a few iterations without human intervention.

DOE Solutions

The analysis of the data shows that, insertion force is the least influential parameter in the assembly process. For the robotic assembly process, it is desirable to reduce the mean cycle time and its variance. After collecting the needed data set using DOE method, the best parameter values recommended by DOE are [300, 35, 75] in Figure 18(d). The corresponding mean cycle time is 3.26s and the standard deviation is $0.19s$.

Results of SVR Enabled Algorithm

The experiments based on SVR were performed online to automatically improve the system performance according to the real-time feedback information. Observed changes resulting in better performance are given with more attention, while changes resulted in worse performance are largely ignored. Compared to the SVR #1 configuration, SVR #2 and SVR #3 divide each parameter into more levels. Thus the underlying relationship between the parameters and the cycle time can be represented more precisely. Due to the variations and noise of the assembly process, the derived SVR models in all experiments are not the same. That is why SVR #2 and SVR #3 experiments converge to two different sets of parameters [300, 30.5, 75] and [300, 30, 75]. However, the discrepancy is very small owing to the model similarity.

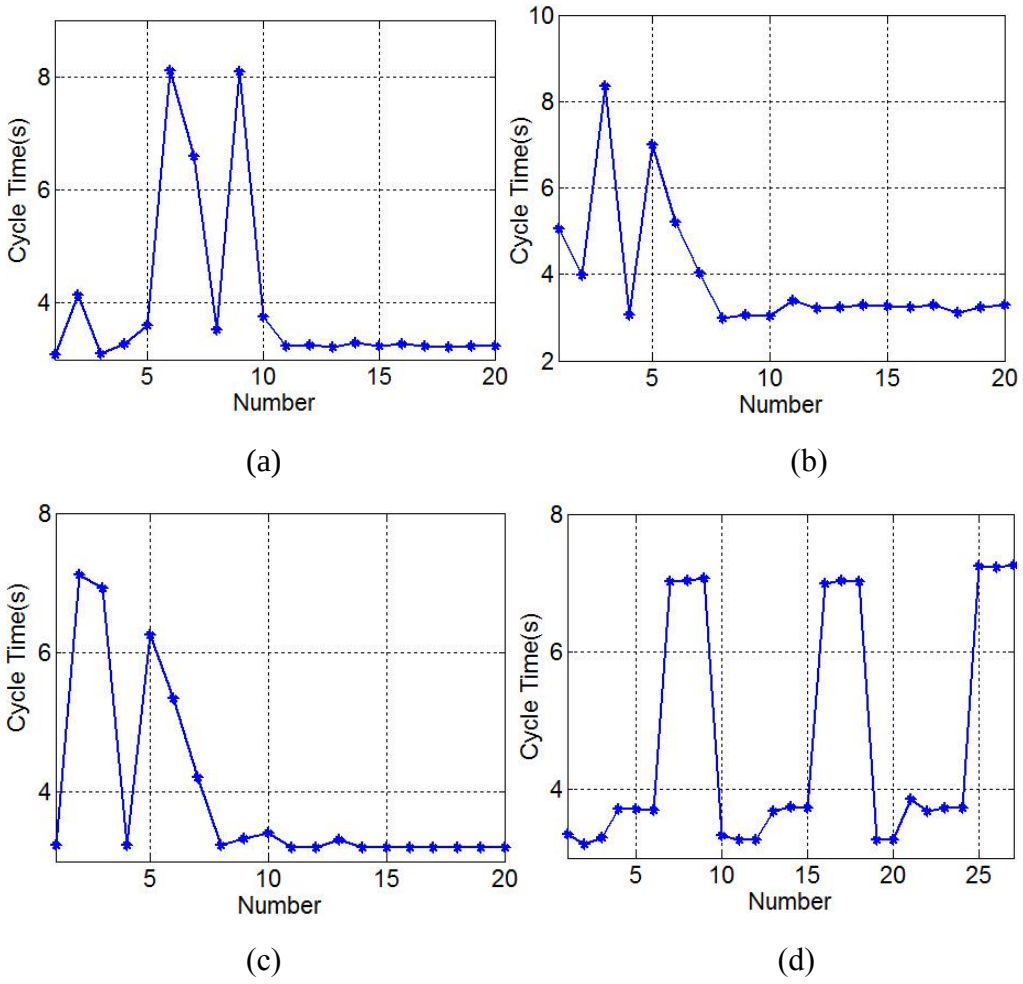

Figure 18. Experiment Results: a) SVR #1. b) SVR #2. c) SVR #3. d) DOE

The three SVR experiments with different configuration are plotted in Figure 18(a), 18(b) and 18(c), respectively. We can see that the initial model is unstable with little useful information. Since this is a continuous self-learning process, the modeling process has a variety of control capabilities, including altering the assembly parameters, switching to the optimization stage to quickly capture the changes of parts and fixtures, and returning to the normal production after parameter adjustment. The proposed method applies SVR enabled parameter optimization in the production to

automatically adapt to the variations in robotic force control assembly and optimize the productivity of the assembly system without disrupting the production. When converging to a minimal point after several iterations, the system still maintains production process under a stable condition.

Each experiment can be divided into two stages: optimization and production. The optimization stage requires 7 to 10 assembly tasks. The algorithm explores the parameter space, constructs the underlying SVR model and finds the optimal process parameters online. With more data sets available, the model is updated step by step. Once the optimal parameters are found, the system switches to the production stage to perform the assembly work using the identified optimal parameters.

Discussion

The optimal assembly parameters, the cycle time (mean and variance) and the number of experiments are listed in Table 13. From Table 13, the number of experiments to identify the optimal assembly parameters is largely reduced by using SVR enabled algorithm.

Table 13. Comparison of Experimental Results

Method	Optimal	μ(s)	$\sigma(s)$	Number of Experiments
SVR #1	[300, 30 ,75]	3.15	0.17	9
SVR #2	[300, 30.5 ,75]	3.20	0.15	7
SVR #3	[300, 32.5 ,75]	3.18	0.13	7
DOE	[300, 35 ,75]	3.26	0.19	810

By comparing the DOE results with that of SVR, it is noted that the SVR enabled

algorithm is able to find the same optimal parameters in only about 10 experiments instead of 810 experiments.

For the DOE method, the assembly parameters cannot be chosen arbitrarily, so the real optimal parameters may not be found. Because the SVR enabled algorithm can explore the interesting area in detail without worrying about the complexity, it can identify the optimal parameters more precisely and achieve better cycle time than DOE based method. Therefore, the SVR is more efficient than the DOE method.

The parameter variations of optimization and production processes of SVR #1 are as shown in Figure 12. Even though the assembly process is influenced by environmental noise, parts variations and locating variations shown (see Figure 19(a) to 19(e)), the process is quite robust in the sense that it finds the optimal parameters and adapts itself to the changing environment. Figure 19(f) and 19(g) are the hyper parameters changes of SVR model before they converge to finish the optimization process. When the SVR enabled algorithm finds the optimal assembly parameters, the switching parameter λ is set to zero to start the production process shown in Figure 19(h).

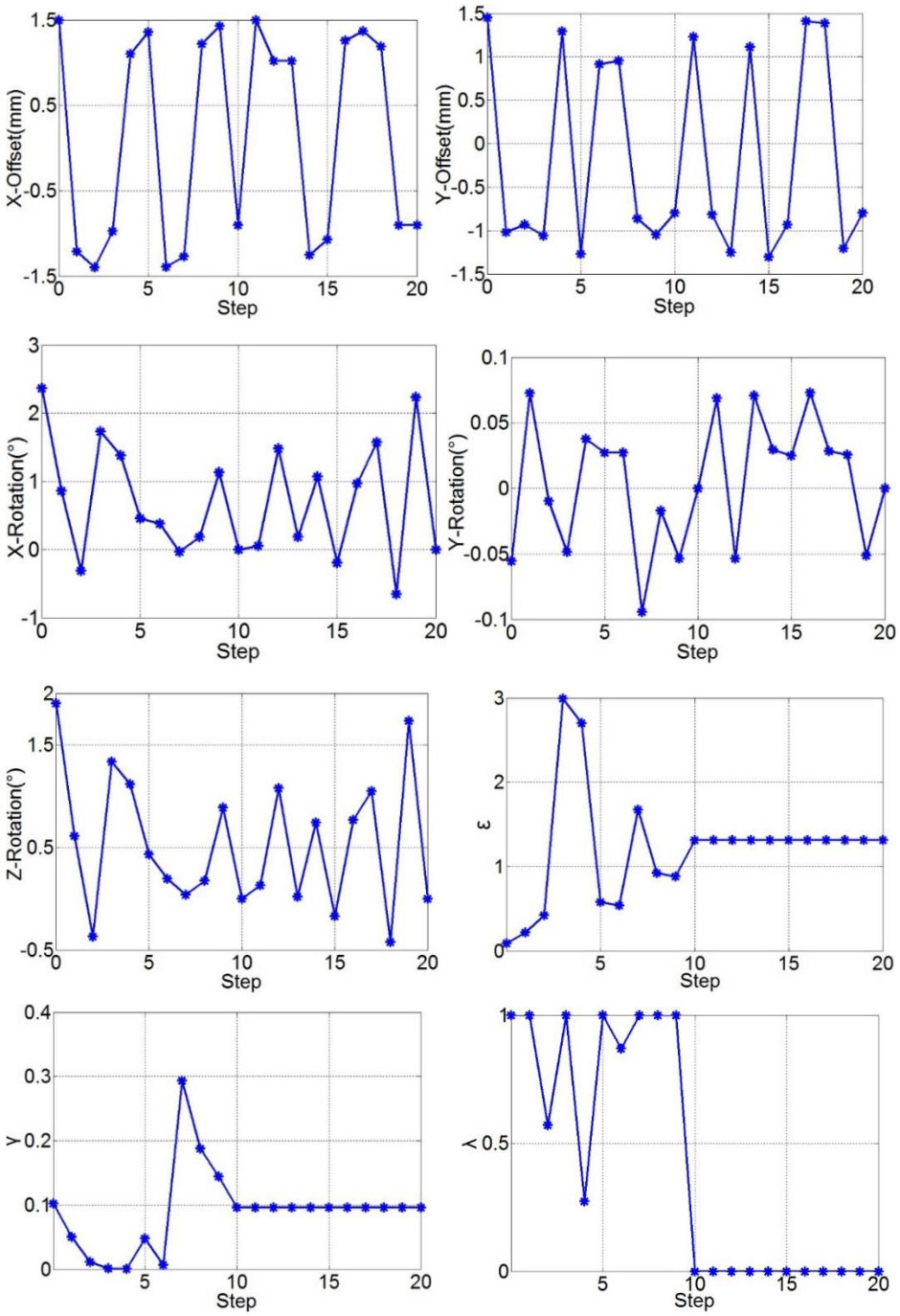

Figure 19. Parameter Variation of SVR 1: a) Random X-Offset of the robot arm axis 6 from the hole position; b) Random Y-Offset of the robot arm axis 6 from the hole position; c) Random X-Axis rotation of the robot arm axis 6; d) Random Y-Axis rotation of the robot arm axis 6; e) Random Z-Axis rotation of the robot arm axis 6; f) Changes of SVR hyper parameter ε step by step, finally converged to 1.3139; g) Changes of SVR hyper parameter γ step by step, finally converged to 0.0961; h) Switching parameter λ

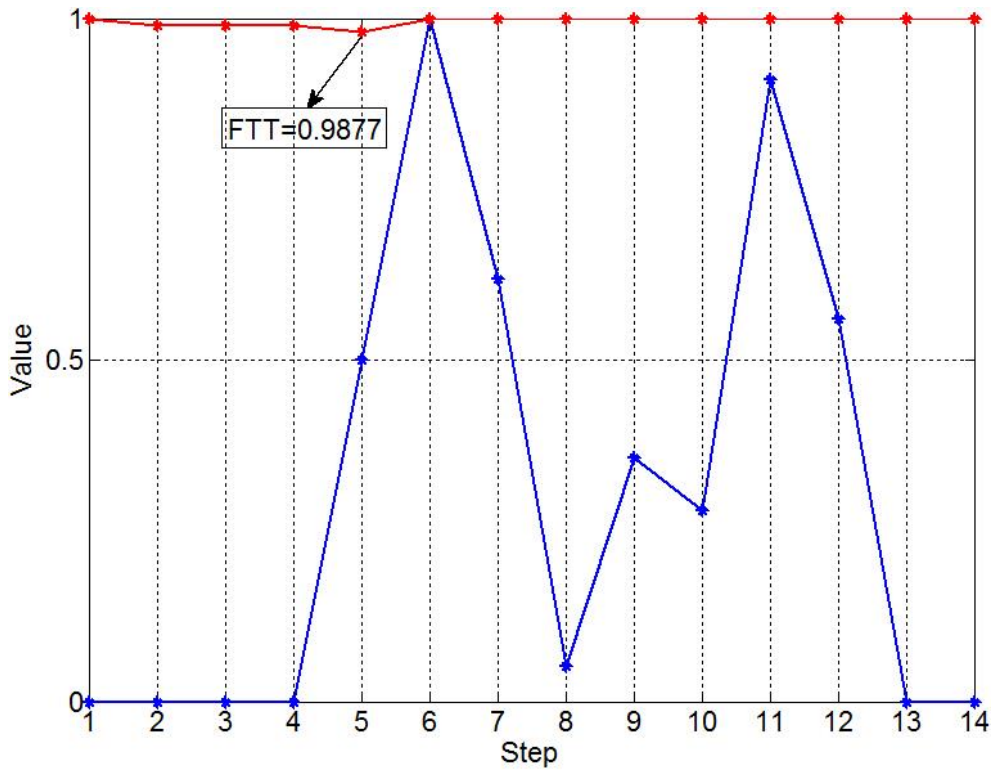

Figure 20. FTT Rate

A special case is examined and the analysis is shown in Figure 20. When the assembly system enters production loop, a piece of sheet steel is placed in front of the hole to block the normal production process with the purpose of restarting the optimization process. Though the peg-in-hole process quitted in the first four assembly processes, the system is able to proceed normally with the identified parameters until the FTT rate drops below 99%. Then λ is set to 0.5 to restart the optimization process. After several search iterations for optimization, the system is stabilized and enters production loop again when λ is set to zero.

DOE methods were chosen and tuned carefully after performing a series of experiments, to obtain the optimal process parameters. The DOE with $3^3 = 27$ sets of parameters were performed offline for comparison. Experiments were repeated 30

times for each set of parameter combination, so there are totally 810 experiments being conducted to minimize the interference from system noise and environmental changes.

CHAPTER VII

PRODUCT-INVENTORY EXPERIMENTAL RESULT

According to the optimized demand response, we solve the production-inventory model by incorporating the proposed load curtailment constraint. In this case, we recomputed the new PI result based on the new solution. Our focus is on the multi-product multi-period under a minimum cost policy, where the production quantity, inventory level and backorders are close linked with each period, however, the total cost is minimized on the whole basis. Two products are produced by only one facility. We also assume that the planning horizon is 52 with one week per period. The experimental result without power response is shown in Table 14.

Table 14. PI Results without Power Response

Week	Product 1			Product 2		
	Production quantity	Inventory level	Backorders	Production quantity	Inventory level	Backorders
1	1353	0	18	489	0	143
2	1094	0	0	662	0	191
3	877	0	0	655	0	0
4	1030	0	0	652	0	0
5	849	0	0	619	0	0
6	908	0	0	522	0	0
7	901	0	0	574	0	0
8	875	0	0	755	134	0
9	1057	0	0	681	0	0
10	833	0	0	787	21	0
11	1100	0	0	658	160	0
12	1119	0	0	645	23	0
13	1156	0	0	621	0	0

Table 14. Continued

Week	Product 1			Product 2		
	Production quantity	Inventory level	Backorders	Production quantity	Inventory level	Backorders
14	997	0	0	620	24	0
15	1094	1	0	662	43	0
16	1269	0	0	545	0	0
17	1008	0	0	677	84	0
18	1094	121	0	662	57	0
19	1145	0	0	628	0	0
20	624	0	0	685	0	0
21	932	0	0	687	47	0
22	1365	0	0	481	0	0
23	929	0	0	643	0	0
24	916	0	0	698	0	0
25	816	0	0	646	17	0
26	1119	0	0	645	0	0
27	684	0	0	644	0	0
28	880	0	0	582	0	0
29	1085	0	0	618	0	0
30	1000	0	0	553	0	0
31	1094	0	0	653	0	0
32	1019	0	0	531	0	0
33	1102	0	0	536	0	0
34	807	0	0	551	0	0
35	1033	0	0	423	0	0
36	765	0	0	686	0	0
37	1117	0	0	620	0	0
38	953	0	0	578	23	0
39	1098	0	0	659	0	0
40	919	0	0	497	0	0
41	1049	0	0	594	0	0
42	1158	0	0	586	0	0

Table 14. Continued

Week	Product 1			Product 2		
	Production quantity	Inventory level	Backorders	Production quantity	Inventory level	Backorders
43	703	0	0	619	0	0
44	720	0	0	619	0	0
45	725	0	0	548	0	0
46	1127	0	0	598	0	0
47	1061	0	0	590	0	0
48	895	0	0	729	91	0
49	1225	0	0	575	0	0
50	1021	0	0	667	0	0
51	762	0	0	548	0	0
52	847	0	0	605	0	0

According to Table 10, the production quantity for each period is different in order to satisfy the constraints. As a consequence, the manufacturing facility would rather bear high level of inventory and backorders in order to lower the cost. For the next stage, we recalculate the PI problem according to the power response. Even though the inventory level and backorders may change as a result, the total production quantity remains the same. The proposed product inventory result with power response is generated in Table 15.

Table 15. PI Results with Power Response

Week	Product 1			Product 2		
	Production quantity	Inventory level	Backorders	Production quantity	Inventory level	Backorders
1	1353	0	18	489	0	143
2	1094	0	0	662	0	191
3	915	38	0	655	0	0
4	1010	18	0	652	0	0
5	831	0	0	619	0	0

Table 15. Continued

Week	Product 1			Product 2		
	Production quantity	Inventory level	Backorders	Production quantity	Inventory level	Backorders
6	908	0	0	522	0	0
7	901	0	0	574	0	0
8	875	0	0	755	134	0
9	1057	0	0	681	0	0
10	833	0	0	787	21	0
11	1100	0	0	658	160	0
12	1119	0	0	645	23	0
13	1156	0	0	621	0	0
14	997	0	0	620	24	0
15	1093	1	0	662	43	0
16	1269	0	0	545	0	0
17	1008	0	0	677	84	0
18	1094	121	0	662	57	0
19	1145	0	0	628	0	0
20	624	0	0	685	0	0
21	932	0	0	687	47	0
22	1365	0	0	481	0	0
23	929	0	0	643	0	0
24	916	0	0	698	0	0
25	816	0	0	655	26	0
26	1134	15	0	636	0	0
27	669	0	0	644	0	0
28	880	0	0	582	0	0
29	1085	0	0	618	0	0
30	1021	21	0	553	0	0
31	1073	0	0	653	0	0
32	1019	0	0	531	0	0
33	1102	0	0	536	0	0
34	807	0	0	551	0	0

Table 15. Continued

Week	Product 2			Product 2		
	Production quantity	Inventory level	Backorders	Production quantity	Inventory level	Backorders
35	1033	0	0	423	0	0
36	765	0	0	686	0	0
37	1117	0	0	620	0	0
38	953	0	0	578	23	0
39	1098	0	0	659	0	0
40	919	0	0	497	0	0
41	1049	0	0	594	0	0
42	1158	0	0	586	0	0
43	703	0	0	619	0	0
44	720	0	0	619	0	0
45	743	18	0	548	0	0
46	1109	0	0	598	0	0
47	1061	0	0	590	0	0
48	895	0	0	743	105	0
49	1245	20	0	561	0	0
50	1001	0	0	667	0	0
51	762	0	0	548	0	0
52	847	0	0	605	0	0

By comparing Tables 7 and 8, we compare the difference in Figure 21, from which we can see that the production quantity for two product remains the level of 51309 and 32008, while the inventory level was changed as 122 to 252 and 724 to 747. Due to higher cost for backorders, the number keeps the same without any changes.

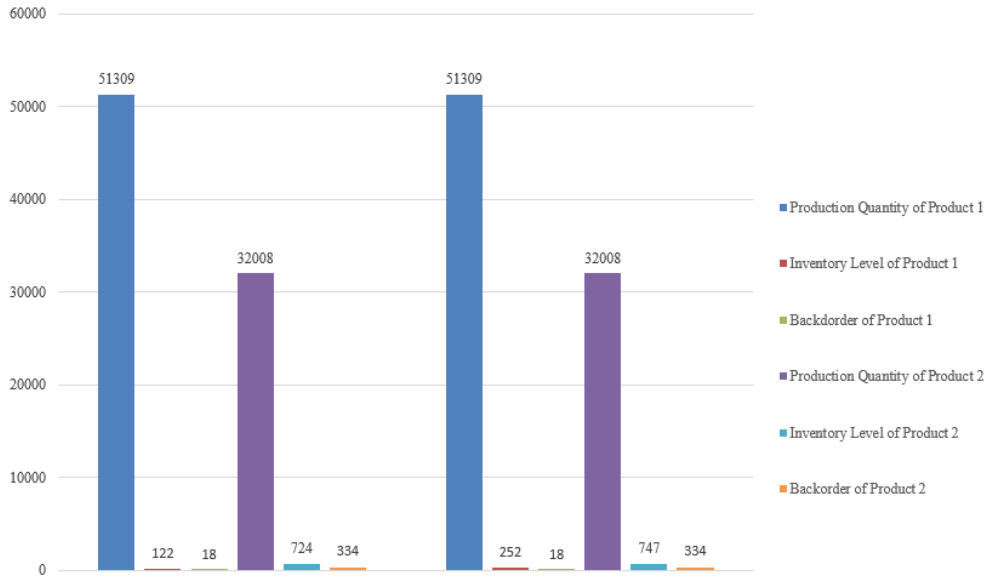

Figure 21. Comparison of Experimental Results

In this step, we solve the proposed product inventory problem to minimize the total cost for manufacturing facility.

CHAPTER VIII

CONCLUSION AND FUTURE WORK

This research fills the gap between the onsite renewable energy sources and energy saving technologies and how they are fused and integrated into the multi-period, production-inventory planning model to realize zero-carbon emission goal for cloud manufacturing. In addition to power intermittency, our model also accommodates the random load curtailments resulted from manufacturer's participation in demand response programs.

Contribution

To decrease electricity usage, an online SVR enabled algorithm is proposed to optimize the process parameters for high precision robotic assembly systems. To demonstrate the effectiveness, we tested the proposed method on a peg-in-hole assembly station in a laboratory setting. The result show that a robot equipped with support vector regression enabled algorithm possesses a strong adaptive capability in uncertain production environments. In short, the SVR enabled algorithm is able to adjust the optimal process parameters online without interrupting the production continuity. Hence, the assembly cycle time is reduced and high FTT rate is guaranteed. These desirable features are obtained as a result of balancing the interactions between exploration and the exploitation.

We also propose a three-stage optimization algorithm to search for the production quantity, the stock level, the backorders, and the generation capacity of wind turbines and solar panels such that the annual production cost is minimized. Different

regions around the world with a variety of climate conditions are used to test the renewables-based production system. We also test out multi-product multi-period product inventory system through rigorous experimental and statistical methods. Albeit the intermittency of wind and solar generation, the results show that it is technically feasible and economically affordable to operate a net-zero carbon production-inventory system via onsite generation scheme.

Future Work

Future investigations in this area are identified as: 1) use real-world manufacturing data to further verify the proposed method; 2) apply the online algorithm to optimize multi-stage robotic assembly processes, such as cylindrical insertion for transmission torque converter assembly; 3) extend the production inventory model for multiple manufacturing factories; 4) include more technologies into the model such as battery storage in industrial applications and vehicle-to-grid service to stabilize the power grid.

REFERENCES

Adams, M. (2003). Green development: Environment and sustainability in the Third World, *Psychology Press*.

Ashok, S. (2006). Peak-load management in steel plants. *Applied energy*. 83(5):413-24.

Brogardh, T. (2007). Present and future robot control developmentan industrial perspective. *Annual Reviews in Control*, vol. 31, no. 1, pp. 69–79.

Bulygina, N. (2007). Model Structure Estimation and Correction Through Data Assimilation. ProQuest.

Zhang, B., Gravel, D., Wang, J., and Bell, A. (2011). Robotic force control assembly parameter optimization for adaptive production. *In 2011 IEEE International Conference on Robotics and Automation (ICRA)*, pp. 464–469.

Li, B., Yu, T., Chen, H., Jin, T. (2015). Manuscript: Toward Net-Zero Carbon Manufacturing Operations: An Onsite Renewables Solution. International Journal of Production Economics.

Carter, C., Corry, M. , Delbanco S., Foster TC-S, Friedland R, Gabel, R. et al. (2010). 2020 vision for a high-quality, high-value maternity care system. *Women's health issues*. 20(1):S7-S17.

Courtney, A., Courtney, M. (2008). Comments Regarding On the Nature of Science. arXiv preprint arXiv:0812.4932.

Chryssolouris, G., Mavrikios, D., Papakostas, N., Mourtzis, D., Michalos, G., Georgoulias, K. (2009). Digital manufacturing: history, perspectives, and outlook. *Proceedings of the Institution of Mechanical Engineers, Part B: Journal of Engineering Manufacture*. 223(5):451-62.

Chao, A. (2008). Optimal policy for a periodic-review inventory system under a supply capacity contract, *Operations Research*, vol. 56, no. 1, pp. 59-68.

Chao, X., Zipkin, P. H. (2010). Optimal policy for a periodic-review inventory system under a supply capacity contract, *Operations Research*. 2010; vol. 56, no. 1, pp. 59-68.

Chen, G., Zhang, L., Arinez, J., Biller, S. (2013). Energy-efficient production systems through schedule-based operations. *IEEE Transactions on Automation Science and Engineering*, 10(1), 27-37.

Choi, C., Xirouchakis, P. (2014). A production planning in highly automated manufacturing system considering multiple process plans with different energy requirements. *The International Journal of Advanced Manufacturing Technology,* 70 (5-8), 853 – 867.

Deif, M. (2011). A system model for green manufacturing. *Journal of Cleaner Production*. 19(14), 1553-1559.

Darnall, N., Jolley, G. J., Handfield, R. (2008). Environmental management systems and green supply chain management: complements for sustainability? *Business Strategy and the Environment.* 17(1):30-45.

Drucker, H., Chris, B., Kaufman, L., Smola, A., Vapnik, V. (1997). Support vector regression machines." *Advances in neural information processing systems*. 9 (1997): 155-161.

Fernandez, M., Li, L., Sun, Z. (2013). "Just-for-Peak" buffer inventory for peak electricity demand reduction of manufacturing systems. *International Journal of Production Economics*. 146(1):178-84.

Federgruen, A. (2013). Approximation of dynamic, multi-location production and inventory Problems. *Management Science*, 30(1), 69-84.

Fernandez, L. (2013). Just-For-Peak buffer inventory for peak electricity demand reduction of manufacturing systems. *International Journal of Production Economics*, pp. vol. 146, no. 1, pp. 178-184.

Fernandez, L. (2013). Just-For-Peak buffer inventory for peak electricity demand reduction of manufacturing systems, *International Journal of Production Economics*, vol. 146, no. 1, pp. 178-184.

Framsyn T. Produktionssystemet-Sveriges Välfärdsmotor. (2003). translated:"The Production system–The Welfare Motor of Sweden"), Stockholm, Sweden, Royal Swedish Academy of Engineering Sciences-IVA.

Gross, R., Leach, M., Bauen, A. (2003). Progress in renewable energy. *Environment International*. 29(1):105-22.

Kampa, M., Castanas, E. (2008). Human health effects of air pollution. *Environmental pollution*. 151(2):362-367.

Kara, S., Manmek, S., Herrmann, C. (2010). Global manufacturing and the embodied energy of products. *CIRP Annals - Manufacturing Technology*. 59(1):29-32.

Karwan, A. (2007). Operations planning with real time pricing of a primary input, *Computers & Operations Research*, pp. 34(3), 848-867.

King, A. A., Lenox, M. J. (2001). Lean and green? An empirical examination of the relationship between lean production and environmental performance, *Production and Operations Management*, vol. 10, no. 3, pp. 244-256.

KiraKusy, M., Rakita, D. (1997). A stochastic linear programming approach to hierarchical production planning. Journal of the Operational Research Society, 48(2), 207 – 211.

Meyer, F., Spröwitz, A., Berthouze, L. (2006). Passive compliance for a rcservo-controlled bouncing robot. *Advanced Robotics*, vol. 20, no. 8, pp. 953–961.

Kleindorfer, R. (2005). Sustainable operations management. *Production and Operations Management*, pp. vo. 14, no. 4, pp. 482-492.

Kesner, S., Howe, R. (2011). Design principles for rapid prototyping forces sensors using 3-d printing. *IEEE/ASME Transactions on Mechatronics*, vol. 16, no. 5, pp. 866–870.

Kim, S., Kim, J. P., Ryu, J. (2014) Adaptive energy-bounding approach for robustly stable interaction control of impedance-controlled industrial robot with uncertain environments. *IEEE/ASME Transactions on Mechatronics*, vol. 19, no. 4, pp. 1195–1205.

Hart S. L. (1995). A natural-resource-based view of the firm. *Academy of management review*,20(4):986-1014.

Higle, A. (2011). Production planning under supply and demand uncertainty: A stochastic programming approach, in: Stochastic Programming". *In International Series in Operations Research & Management Science (pp. 297–315).* New York: Springer.

Ierapetritou, G. (2002). Cost minimization in an energy-intensive plant using mathematical programming approaches. *Industrial and Engineering Chemistry Research*, pp. 41(21), 5262–5277.

Kohavi, R. (1995). A study of cross-validation and bootstrap for accuracy estimation and model selection. *In IJCAI*, vol. 14, no. 2, pp. 1137-1145.

Lieberman B., Montgomery B. (1988). First mover advantages. *Strategic management journal.* 9(S1):41-58.

Lund, H. (2007). Renewable energy strategies for sustainable development. *Energy*. *32*(6), 912-919.

Lund, H. (2006). Large-scale integration of optimal combinations of PV, wind and wave power into the electricity supply, *Renewable Energy*. 31(4):503-15.

Lund, H., Kempton, W. (2008). Integration of renewable energy into the transport and electricity sectors through V2G, *Energy policy*. 36(9):3578-87.

Lee, A. (1988). Production control in multistage systems with variable yield losses. *Operations Research*, 36(2), 269-279, 1988.

Lin, A. (2013). Dynamic energy control for energy efficiency improvement of sustainable manufacturing systems using Markov decision process. *IEEE Transactions on Systems, Man and Cybernetics: Systems*, pp. 43(5), 1195-1205.

Lasserre, B. (2001). Global optimization with polynomials and the problem of moments. *SIAM Journal on Optimization*. 11.3 (2001): 796-817.

Lai, L., El Gamal, H., Jiang, H., & Poor, H. V. (2011). Cognitive medium access: Exploration, exploitation, and competition. *IEEE Transactions on Computing Mobile*, 10, no. 2 (2011): 239-253.

Meier, H., Roy, R., Seliger, G. (2010). Industrial Product-Service Systems—IPS 2. *CIRP Annals-Manufacturing Technology.* 59(2):607-27.

Mell, P., Grance, T. (2011). The NIST definition of cloud computing (draft). *NIST special publication*. 800(145):7.

McDonough, W., Braungart, M., Anastas, T., Zimmerman, B. (2003). Applying the principles of green engineering to cradle-to-cradle design. *Environmental science & technology.* 37(23):434A-441A.

Mitsuishi, M., Nagao, T. (1999). Networked Manufacturing with Reality Sensation for Technology Transfer. *CIRP Annals - Manufacturing Technology.* 48(1):409-12.

Mitra, S., Grossmann, E., Pinto, J. M., Arora, N. (2012). Optimal production planning under time-sensitive electricity prices for continuous power-intensive processes. *Computer and Chemical Engineering*, vol. 38, no. 5, pp. 171-184.

Moonand, J., Park, J. Y. (2014) Smart production scheduling with time-dependent and machine-dependent electricity cost by considering distributed energy resources and energy storage. *International Journal of Production Research*, vol. 52, no. 13, pp. 3922-3939.

Mouzon, M. (2007). Operational methods for minimization of energy consumption of manufacturing equipment. *International Journal of Production Research*, pp. vol. 45, no. 18-19, pp. 4247-4271.

Meyer, F., Alexander S., Luc B. (2006). Passive compliance for a RC servo-controlled bouncing robot. *Advanced Robotics 20*, no. 8: 953-961.

Marvel, A., Wyatt S. N., Dave P. G., George, Z., Jianjun, W., Tom, F. (2008). Automated learning for parameter optimization of robotic assembly tasks utilizing genetic algorithms. *IEEE International Conference on Robotics and Biomimetics*, pp. 179-184.

Mattera, D., Simon H. (1999). Support vector machines for dynamic reconstruction of a chaotic system." *In Advances in kernel methods*, pp. 211-241. MIT Press.

Ostring, M. (2002). Identification, diagnosis, and control of a flexible robot arm. Division of Automatic Control, Department of Electrical Engineering, Linkopings universitet.

Marvel, A., Wyatt S. N. (2009). Accelerating robotic assembly parameter optimization through the generation of internal models. *In 2009 IEEE International Conference on Technologies for Practical Robot Applications*, pp. 42-47.

Ning, W., Zhang, F., Yin, Q., Ni, X. (2011). The architecture of cloud maufacturing and its key technologies research. *IEEE International Conference on Cloud Computing and Intelligence Systems (CCIS)*. 259-263.

Marvel, J., Newman, W., Gravel, W, Zhang., G, Wang., J, Fuhlbrigge, T. (2008) Automated learning for parameter optimization of robotic assembly tasks utilizing genetic algorithms. *In IEEE International Conference on Robotics and Biomimetics*, pp. 179–184.

Marvel, J., Newman, W. (2011). Model-assisted stochastic learning for robotic applications. *IEEE Transactions on Automation Science and Engineering*, vol. 8, no. 4, pp. 835–845.

Nam, K., Fujimoto, H., Hori, Y. (2014). Advanced motion control of electric vehicles based on robust lateral tire force control via active front steering. *IEEE/ASME Transactions on Mechatronics*, vol. 19, no. 1, pp. 289–299.

Omer, M. (2008). Green energies and the environment. R*enewable and Sustainable Energy Reviews*, 12(7):1789-821.

Ostring, M. (2002). Identification, diagnosis, and control of a flexible robot arm. Division of Automatic Control, Department of Electrical Engineering,Linkopings universitet.

Porter, E., Van, C. (1995). Green and competitive: ending the stalemate. *Harvard business review*. 1995;73(5):120-134.

Sawhney, R,, Teparakul, P., Bagchi, A., Li, X. (2007). En-Lean: a framework to align lean and green manufacturing in the metal cutting supply chain. *International Journal of Enterprise Network Management.* 1(3):238-260.

Salcedo-Sanz, S., Ortiz-Garcı, E. G., Pérez-Bellido, Á. M., Portilla-Figueras, A., Prieto, L. (2011). Short term wind speed prediction based on evolutionary support vector regression algorithms. *Expert Systems with Applications* 38.4 (2011): 4052-4057.

Sharifi, H., Colquhoun, G., Barclay, I., Dann, Z. (2001). Agile manufacturing: a management and operational framework. *Proceedings of the Institution of Mechanical Engineers, Part B: Journal of Engineering Manufacture*. 215(6):857-869.

Sangwan, S. (2006). Performance value analysis for justification of green manufacturing systems. *Journal of Advanced Manufacturing Systems*. 5(01):59-73.

Solangi, H., Islam, R., Saidur, R., Rahim, A., Fayaz, H. (2011). A review on global solar energy policy, *Renewable and Sustainable Energy Reviews*. 15(4):2149-63

Smola, J., Schölkopf, B. (2004). A tutorial on support vector regression. *Statistics and computing.* 14.3 (2004): 199-222.

Suykens, K., Vandewalle, J., Moor, B. (2001). Optimal control by least squares support vector machines. *Neural Networks* 14, no. 1 (2001): 23-35.

Tao, F., Zhang, L., Nee, A. Y. C. (2011). A review of the application of grid technology in manufacturing. *International Journal of Production Research.* 49(13):4119-55.

The New York Times. (2012). Skilled Work , Without the Worker, avaliable: http://www.nytimes.com/2012/08/19/business/new-wave-of-adept-robots-is-changing-global-industry.html (accessed on March 31, 2015)

Jin, T., Jimenez, J., & Tian, Z. (2013, August). Managing demand response for manufacturing enterprises via renewable energy integration. *2013 IEEE International Conference on utomation Science and Engineering*, pp. 645-650.

Udomleartprasert, P. (2004). Roadmap to green supply chain electronics: design for manufacturing implementation and management. *Proceedings of 2004 International IEEE Conference on the Asian Green Electronics*, 169-173.

Vapnik, V., Golowich, S. E., Smola, A. (1997). Support vector method for function approximation, regression estimation, and signal processing. *Advances in neural information processing systems*, 281-287.

Wu, D., Greer, M. J., Rosen, D. W., Schaefer, D. (2013). Cloud manufacturing: Strategic vision and state-of-the-art, *Journal of Manufacturing Systems*, 32(4), 564-579.

Wang, K., Timon, D. (2014). Implementing support vector regression with differential evolution to forecast motherboard shipments. *Expert Systems with Applications* 41.8 (2014): 3850-3855.

Vaaler, E., Seering, W. (1991). A machine learning algorithm for automated assembly. *In IEEE International Conference on Robotics and Automation*, pp. 2231–2237.

Xu, X. (2012). From cloud computing to cloud manufacturing. *Robotics and computer-integrated manufacturing*. 28(1):75-86.

Xu, Q. (2013). Precision position/force interaction control of a piezoelectric multimorph microgripper for microassembly. IEEE Transactions on Automation Science and Engineering, vol. 10, no. 3, pp. 503–514.

Zhang, X., (2000). Introduction to statistical learning theory and support vector machines. *Acta Automatica Sinica* 26, no. 1 (2000): 32-42.

Yu, S., Chen, T., Chang, F. (2006). Support vector regression for real-time flood stage forecasting. *Journal of Hydrology* 328.3 (2006): 704-716.

Zhang, B., Gravel, D., Wang, J., Bell, A. (2011). Robotic force control assembly parameter optimization for adaptive production. *In 2011 IEEE International Conference on Robotics and Automation*, pp. 464-469.